

# **IMPACT OF ANTENNA ARRAY GEOMETRY ON THE CAPACITY OF MIMO COMMUNICATION SYSTEM**

Muhammad Tanvir Hassan

Student ID: 06310044

S.M. Nurul Morshed

Student ID: 06210026

Mahbub-UI-Alam

Student ID: 07310090

**Department of Computer Science and Engineering  
September 2007**



**BRAC University, Dhaka, Bangladesh**

## **Abstract**

More services and higher data rates are the demands of future wireless communication system end users. In order to accommodate these expectations while maintaining robustness against wireless impairments, contemporary technologies have to be developed. Multiple-input multiple-output (MIMO) techniques stand as a strong candidate to allow robustness against channel fading and interference as well as to enable high data rates.

This dissertation investigates the impact of different array geometries on the capacity of MIMO communication systems. Five different array configurations, Uniform Linear Array, Non-Uniform Linear Array, Uniform Circular Array, Hexagonal Array and Star Array, are being used to compare their performance from capacity point of view. The expression of the capacity of a MIMO communication system is derived from an information-theoretic approach and is altered to introduce the impact of array geometry on the system capacity. Using this expression the capacities of MIMO systems with different array geometries are compared. Also the impact of increasing the number of element of the array and changing the inter-element spacing of the array elements are examined. The significant increase in achievable capacity using array of antennas at both end of the transmission link is observed to justify the ascendancy of MIMO system.

# Contents

Abstract	2
List of Figure	5
List of Abbreviations	6
<b>1 Introduction</b>	<b>7</b>
1.1 MIMO System	8
1.2 Reasons Behind the Improved Performance of MIMO Systems .	10
1.2.1 Array Gain	10
1.2.2 Diversity Gain	10
1.2.3 Spatial Multiplexing Gain	11
1.2.4 Interference Reduction	11
1.3 Arrangement of Antennas in MIMO Systems	11
1.3.1 Multiple Antenna Systems	11
1.3.2 Antenna Array Systems	12
<b>2 Capacity of MIMO Communication System</b>	<b>13</b>
2.1 Derivation of the Expression of Capacity for MIMO System	14
2.2 Model for the Wireless Channel	14
2.3 Expression of the Capacity	15
<b>3 Impact of Antenna Array Geometry</b>	<b>23</b>
3.1 Array of Antennas	23
3.2 Concept of Manifold Vector	24
3.3 Impact of Manifold Vector on System Capacity	30
3.3.1 Impact of Manifold Vector	30
3.3.2 Channel Matrix Considering Antenna Array Geometry	31

3.4 Expression of Capacity Considering Array Geometry	33
<b>4 Simulation Results</b>	<b>34</b>
4.1 General Scenario for the Simulations	35
4.2 SIVO System Without Using Beamforming Techniques	36
4.2.1 Impact of SNR and Angle of Arrival (AoA) on Capacity	37
4.2.2 Impact of Number of Array Elements on Capacity	42
4.2.3 Comments on Simulation Results	44
<b>5 Conclusions and Future Works</b>	<b>44</b>
A Antenna Array Geometries used in the Simulation	51
B Simulation Codes	54
B.1 Code for array manifold vector	54
B.2 Code for Section 4.2.1	54
code for section 4.2.2	60
B.3 code for ULA	60
B.4 code for UCA	65
B.5 code for HA	70

# List of Figure:

Figure 1.1: MIMO wireless system	9
Figure 1.2: MIMO system with transmitter and receiver using Antenna array	13
Figure 3.1: Relative geometry between a far-field emitting source And array of sensors	25
Figure 3.2: Geometry of traveling spherical wave, relative to The k-th sensor and the array reference point	28
Figure 3.3: Scenario for multiple source detection with MIMO system	31
Figure 3.4: SIVO Channel Model	33
Figure 4.1: General Scenario for Simulations	36
Figure 4.2: Impact of Different Antenna Geometry on Capacity For SIVO Systems	37
Figure 4.3: Variation in System Capacity Using Uniform Linear Array	39
Figure 4.4: Variation in System Capacity Using Non-Uniform Linear Array	40
Figure 4.5: Variation in System Capacity Using Uniform Circular Array	40
Figure 5.6: Variation in System Capacity Using Hexagonal Array	41
Figure 5.7: Variation in System Capacity Using Star Array	41
Figure 4.8: Change in Capacity with change in Number of Array Elements for Uniform Linear Array	42
Figure 4.9: Change in Capacity with change in Number of Array Elements for Uniform Circular Array	43
Figure 4.10: Change in Capacity with change in Number of Array Elements for Star Array	43

# List of Abbreviations and Acronyms

AWGN	Additive White Gaussian Noise
MIMO	Multiple Input Multiple Output
BW	Bandwidth
MEA	Multi Element Array
CSI	Channel State Information
SIMO	Single Input Multiple Output
MISO	Multiple Input Single Output
NLOS	Non Line of Sight
SNR	Signal to Noise Ratio
SIVO	Single Input Vector Output
VIVO	Vector Input Vector Output
DOA	Direction of Arrival
TOA	Time of Arrival
ULA	Uniform Linear Array
NULA	Non Uniform Linear Array
UCA	Uniform Circular Array
HA	Hexagonal Array
StA	Star Array
WLAN	Wireless Local Area Network
WWAN	Wireless Wide Area Network
SNIR	Signal to Noise plus Interference Ratio
SS	Spread Spectrum
STAR	Space-Time Arrayed

# Chapter 1

## Introduction

Research on wireless communication systems is currently of significant interest in the communication society. While the first and second generations of wireless systems focus on voice communications, current research focuses mainly on providing both voice and data access. In recent years, while the quality and data rate provided by wireless systems increased rapidly and became comparable to their wire line counterparts, the flexibility in wireless systems made it possible to develop a rich collection of new wireless data applications, which promises to have great impact on people's daily life. The increasing demand for high-speed, high-quality mobile communication has fueled interest in spectrum-efficient multiple-input multiple-output (MIMO) wireless communication links [21, 22]. Systems with MIMO communication links use multiple antenna arrays, one at the transmitter and one at the receiver, to take full advantage of the spatial dimension of the propagation channel. When properly designed, multi-array communication links can provide multi-fold increases in link throughput in addition to dramatic reductions in channel variation. This can be used to provide higher data rates to single users, lower delay links, or to allow multiple users to coexist in the spatial channel. Due to these advantages, MIMO capability is being considered for all candidate wireless networks including wireless local area networks [23,24], third generation mobile cellular systems [25,28], and fourth generation mobile cellular systems [29].

Recent researches have demonstrated that the capacity of most wireless signals can be significantly increased by making use of spatial diversity [2], [3], [4], [14]. To overcome the problem of limited bandwidth (BW), multiple antennas can be employed in one or both side of the transmission link. Multi-antenna structures

will thus be in the form of single input multiple outputs (SIMO), multiple inputs single output (MISO), or multiple inputs multiple outputs (MIMO). If the propagation medium is rich scattering, a MIMO structure can attain much greater capacity than SIMO/MISO structures. To achieve this increased capacity no increase in BW or transmitted power is required. The ability of achieving this capacity is influenced by the available channel information at either the receiver or transmitter, channel environment, geometry of arrays used and the correlation between the channel gains on each antenna element [19].

Use of array of antennas at both ends of the transmission link, provide significant increase in the achievable capacity in MIMO system. The ability of achieving this high capacity is greatly influenced by the geometry of antenna array used and the correlation between the channel gains on each antenna element in the array. In this paper, the impact of different array configurations on the system capacity is observed and compared. Five different array configurations - Uniform linear array, Non-uniform linear array, Uniform circular array, Hexagonal array and Star array are used to compare their performances.

### **1.1 MIMO System**

More services and higher data rates are the demands of future wireless communication system end users. In order to accommodate these expectations while maintaining robustness against wireless impairments, contemporary technologies have to be developed. Multiple-input multiple-output (MIMO) techniques stand as a strong candidate to allow robustness against channel fading and interference as well as to enable high data rates [26,27]. However, the performance of future MIMO wireless communication systems strongly depends on the propagation environment and the antenna array configuration [30][31]. Recently, in [21,22] the impact of five antenna array geometries on wireless MIMO system performance has been studied using the clustered channel model [33] in indoor scenario. It is shown in [32] that in low spatial correlation

environment the ULA geometry outperforms the other considered array geometries in terms of channel capacity and bit error rate performance. In [14] a compact MIMO antenna array was proposed by combining polarization diversity and space diversity into one arrangement consisting of a cube. It is shown that even for very small inter-element spacing considerable capacity is obtained due to polarization diversity.

The performance of MIMO wireless communication systems highly depends on the propagation environment, antenna array geometry and the antenna element properties. In previous work we have studied the influence of environment physical parameters on the capacity of outdoor MIMO channel [35]. Parameters such as street width, wall relative permittivity and reflection order were considered.

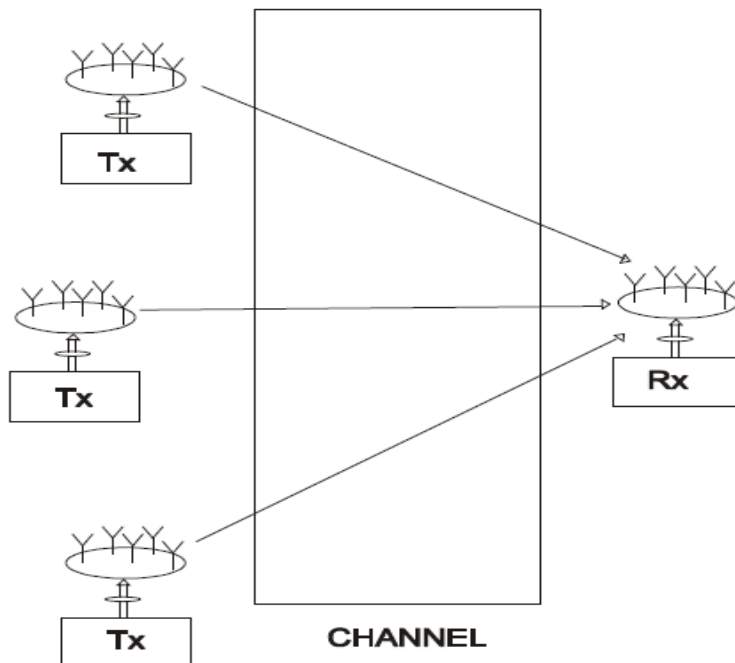


Figure 1.1: MIMO Wireless System

## **1.2 Reasons Behind the Improved Performance of MIMO Systems**

The performance improvements resulting from the use of MIMO systems are due to array gain, diversity gain, spatial multiplexing gain and interference reduction.

### **1.2.1 Array Gain**

In MIMO communication systems, array gain means a power gain of transmitted signals that is achieved by using multiple-antennas at transmitter and/or receiver. Array gain results in an increase in average SNR due to a coherent combining effect. Transmit/receive array gain requires channel knowledge in the transmitter and receiver respectively. It also depends on the number of transmit and receive antennas. Channel knowledge at the receiver is typically available whereas channel state information at the transmitter is in general more difficult to maintain.

### **1.2.2 Diversity Gain**

Diversity is a powerful technique to mitigate fading in wireless links. It is the increase in signal-to-interference ratio due to some diversity scheme, or how much the transmission power can be reduced when a diversity scheme is introduced, without a performance loss. Diversity leads to improved link reliability by rendering the channel “less fading” and by increasing the robustness to co-channel interference. Diversity gain is obtained by transmitting the data signal over multiple (ideally) independently fading dimensions in time, frequency, and space and by performing proper combining in the receiver. Spatial (i.e., antenna) diversity is particularly attractive when compared to time or frequency diversity, as it does not incur expenditure in transmission time or bandwidth, respectively. Space-time coding [5] realizes spatial diversity gain in systems with multiple transmit antennas without requiring channel knowledge at the transmitter.

### **1.2.3 Spatial Multiplexing Gain**

MIMO channels offer a linear increase in capacity for no additional power or bandwidth expenditure. This gain, referred to as spatial multiplexing gain, is realized by transmitting independent data signals from the individual antennas. Under conducive channel conditions, such as rich scattering, the receiver can separate the different streams, yielding a linear increase in capacity.

### **1.2.4 Interference Reduction**

When multiple antennas are used, the differentiation between the spatial signatures of the desired signal and co-channel signals can be exploited to reduce interference. Interference reduction requires knowledge of the desired signal's channel. Interference reduction can also be implemented at the transmitter, where the goal is to minimize the interference energy sent toward the co-channel users while delivering the signal to the desired user. Interference reduction allows aggressive frequency reuse and thereby increases multi-cell capacity.

## **1.3 Arrangement of Antennas in MIMO Systems**

A MIMO system is defined as a system employing antenna elements at both ends of the transmission link. The arrangement of antennas is of great importance in MIMO systems. Two usually used forms depending on the spacing between antenna elements are multiple antenna system and antenna array system.

### **1.3.1 Multiple Antenna Systems**

The spacing between antennas elements significantly influences the correlation between the signals at different array elements. The farther the elements are spaced, the lower the correlation between the signals received at each antenna. When the elements are sufficiently spaced, the signals decorrelate from one element to the other enabling to realize antenna diversity. Diversity gain allows

reduction in average output SNR per antenna for a given bit error rate. When the elements are closely packed, directional gain helps to reduce the required received signal power for a given output SNR. The use of multiple antennas at both end of the transmission link produces significant performance improvements, including the reduction of bit error rates and the increase in system capacity [15]. These improvements allow more users to access the system with higher data rates for the same bit error rates than in the case of single antenna. But this form of antenna arrangement fails to suppress multiple access interference.

### **1.3.2 Antenna Array Systems**

An array system is a collection of antennas, which are spatially distributed at judicious locations in the 3-dimensional real space, with a common reference point [6]. By making use of the spatio-temporal properties of the channel provided by the antenna array, an extra layer of co-channel interference cancellation and new ways for handling unwanted signal effects can be developed. The temporal and spatial signal structure induced by the multi-paths and the geometry of multiple receiving antennas can be usefully exploited for interference suppression. The geometry of the array plays an important role in the improvement of performance of the system. Researchers for different scenarios have worked different antenna geometry on. In the array system, the whole array is taken into consideration as a single identity and the spatio-temporal property induced by the geometry of the array helps the capacity of the system to increase significantly [9].

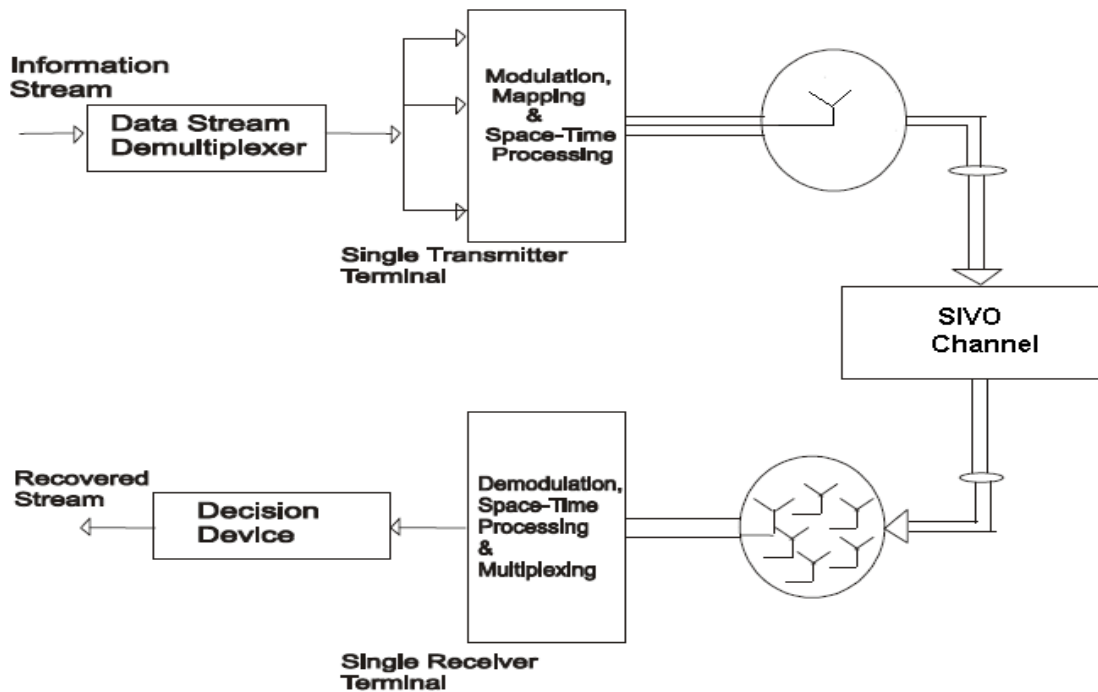


Figure 1.2: MIMO System with Transmitter and Receiver using Antenna Array

## Chapter 2

### Capacity of MIMO Communication System

Information theory started with Shannon's paper .A Mathematical Theory of Communication published in 1948 [1], which also founded the modern theory of communication. Before 1995, the mainstream of wireless communication research focused on improving radio link reliability and capacity motivated by Shannon's work. The field changed around 1995, when the seminal papers by Fochini [2], [3] and Teletar [4] independently showed that in a rich scattering environment, the capacity of a point to point wireless link can be greatly increased by employing multi element antenna arrays at both end of the link. The underlying transmission link is referred as a MIMO channel. In this dissertation an information-theoretic approach (same approach was taken by [8] and [18]) is

taken to investigate, for a fading environment, the value of using a substantial number of antenna elements at both transmitter and receiver.

## **2.1 Derivation of the Expression of Capacity for MIMO System**

In this dissertation focus is given to investigate, for a fading environment, the value of using a substantial number of antenna elements at both transmitter and receiver. The analysis is conducted in an idealized context for a quasi-static channel. The channel bandwidth and transmitted power is being constrained and it is shown that by forming a channel using increased spatial dimensions one can get extraordinarily large capacity. The transmitter does not know the channel characteristic but the receiver knows (estimates by tracking) the characteristic which is subject to Rayleigh fading. For a scenario where the transmitter has the channel state information (CSI), a fast feedback link is required. But the time it takes for the feedback link to inform the transmitter the CSI, contradicts the assumption of quasi-static channel. The analysis is restricted to narrowband case where the bandwidth is taken to be narrow enough that the channel can be treated as flat over frequency and we express capacity in units of bps/Hz. An environment with large number of scatterers is assumed so that the Rayleigh fading model is appropriate. The assumption of independent Rayleigh paths make sure that for antenna elements placed on a rectangular lattice with half wavelength spacing, the path losses roughly tend to decorrelate [2]. The noise is assumed to be additive white Gaussian noise (AWGN).

## **2.2 Model for the Wireless Channel**

Consider a single user Gaussian channel for point to point communication with AWGN. The time is taken to be discrete. The basic setup of the channel under consideration is given below.

- a. Number of antenna at the transmitter,  $M$

- b. Number of antenna at the receiver,  $N$
- c. Transmitted signal,  $m(t)$ , is  $M$  dimensional. The total power is constrained to  $P_s$  regardless of the value of  $M$ .
- d. The bandwidth is narrow enough that we can treat the channel as frequency at fading.
- e. The noise at the receiver,  $n(t)$ , is complex  $N$  dimensional AWGN with statistically independent power  $P_n$  each of the  $N$  receiving antennas.
- f. The received signal,  $x(t)$ , is  $N$  dimensional so that at each point in time there is one complex vector component per receive antenna.
- g. When there is only one transmit antenna, it radiates power  $P_s$  and the average power at the output of each of the receiving antennas is  $P$ .
- h. The channel matrix,  $H$ , is Rayleigh distributed with complex, zero mean and unit variance.

### **2.3 Expression of the Capacity**

The theoretical upper limit to the performance of a communications system was given by Shannon as an upper bound to the maximum rate at which information can be transmitted over a communication channel. This rate is called the channel capacity. According to Shannon's capacity theorem, it is the maximum possible mutual information that can be achieved through a communication link. The

maximum is taken over all possible distribution of the input to the communication link. So the capacity of a communication channel,

$$C = \max\{I(\underline{X}; \underline{m}(t))\} \quad (2,1)$$

Here,  $I(\underline{X}; \underline{m}(t))$  is the mutual information between the transmitted and received signal. According to the definition of mutual information,  $I(\underline{X}; \underline{m}(t))$  can be expressed in terms of the entropies of  $\underline{X}$  and  $\underline{m}(t)$ ,

$$I(\underline{X}; \underline{m}(t)) = h(\underline{X}) - h(\underline{X} | \underline{m}(t)) \quad (2,2)$$

Using the expression of mutual information from Equ. 2.2, Equ. 2.1 can be expressed as,

$$C = \max\{h(\underline{X}) - h(\underline{X} | \underline{m}(t))\} \quad (2,3)$$

Where the differential entropy of a continuous random variable  $X$  with a density  $f(x)$  is given by,

$$h(\underline{X}) = - \int f(x) \log f(x) dx \quad (2,4)$$

For a Gaussian channel with AWGN the received signal is the summation of the transmitted signal and the noise. So the Eqn. 2.3 becomes,

$$C = \max\{h(\underline{X}) - h(\underline{m}(t) + \underline{n}(t) | \underline{m}(t))\} \quad (2,5)$$

As translation does not change differential entropy and the noise is independent of the transmitted signal, we have,

$$C = \max\{h(\underline{X}) - h(\underline{n}(t))\} \quad (2,6)$$

The noise is assumed to be additive white gaussian. So the entropy of noise is the entropy of a gaussian distributed variable (the proof of this expression of entropy of a gaussian random variable is given in the appendix [A] ),

$$h(\underline{n}(t)) = \frac{1}{2} \log_2(2\pi e)^n |\mathbb{R}_{nn}| \quad (2,7)$$

where,  $\mathbb{R}_{nn}$  is the covariance matrix of  $\underline{n}(t)$ . So the Equ. 2.6 can be expressed as,

$$\begin{aligned}
C &= \max\{h(\underline{X}) - \frac{1}{2} \log_2(2\Pi e)^n |\mathbb{R}_{nn}|\}\} \\
&= \max\{h(\underline{X})\} - \frac{1}{2} \log_2(2\Pi e)^n |\mathbb{R}_{nn}|
\end{aligned}$$

So the expression of capacity, assuming that the noise is AWGN, is,

$$C = \max\{h(\underline{X})\} - \frac{1}{2} \log_2(2\Pi e)^n |\mathbb{R}_{nn}| \quad (2.8)$$

The above expression leaves us to find the distribution of X that maximizes its entropy and hence capacity of the system. To find out the distribution that maximizes the entropy, let, Y be a random vector with zero mean and covariance

$$\mathbb{R} = E\{\underline{Y} \cdot \underline{Y}^T\}$$

g(y) be any density function satisfying,

$$\int g(\underline{y}) \cdot y_i \cdot y_j \, d\underline{y} = R_{ij}$$

$\phi_k$  be the density function of a gaussian distributed random variable  $\sim N(0; \mathbb{R})$ , with

$$\phi_k = \frac{1}{(\sqrt{2\pi})^n} \exp\left(-\frac{1}{2} \underline{Y}^T \cdot \mathbb{R}^{-1} \cdot \underline{Y}\right) \quad (2.9)$$

So the entropy of  $\Phi_k$  as mentioned above for a Gaussian distributed random variable,

$$h(\phi_k) = \frac{1}{2} \log_2(2\pi e)^n |\mathbb{R}| \quad (2,10)$$

According to Information inequality, the relative entropy is always positive [8]. So,

$$\begin{aligned} 0 &\leq D(g||\phi_k) \\ &\leq \int g \log_2(g/\phi_k) \\ &\leq \int g \log_2 g - \int g \log_2 \phi_k \\ &\leq -h(g) - \int g \log_2 \phi_k \\ &\leq -h(g) + h(\phi_k) \end{aligned}$$

So the Gaussian distribution maximizes the entropy over all distributions with the same covariance.

$$h(g) \leq h(\phi_k) \quad (2,11)$$

Using the value of in Eqn.2.10 in Eqn.2.11,

$$h(g) \leq \frac{1}{2} \log_2(2\pi e)^n |\mathbb{R}|$$

This allows us to find the maximum entropy,

$$\max\{h(\underline{X})\} = \frac{1}{2} \log_2(2\pi e)^n |\mathbb{R}_{xx}| \quad (2,12)$$

Putting the value of  $\max\{h(\underline{X})\}$  in Eqn. 2.8, we have,

$$\begin{aligned} C &= \frac{1}{2} \log_2(2\pi e)^n |\mathbb{R}_{xx}| - \frac{1}{2} \log_2(2\pi e)^n |\mathbb{R}_{nn}| \\ &= \frac{1}{2} \log_2 \frac{|\mathbb{R}_{xx}|}{|\mathbb{R}_{nn}|} \end{aligned}$$

So capacity can be expressed as a function of covariance matrices of the received signal and the noise as,

$$C = \frac{1}{2} \log_2 \frac{|\mathbb{R}_{xx}|}{|\mathbb{R}_{nn}|} \quad (2,13)$$

where,  $\mathbb{R}_{xx}$  is the covariance matrix of  $\underline{X}(t)$ . Now to find the expression of the covariance matrices of the received signal and the noise, expression of the received signal can be used. The basic vector equation describing the channel operating on the transmitted signal  $\underline{m}(t)$  is,

$$\begin{aligned} \underline{x}(t) &= \mathbb{H} \cdot \underline{m}(t) + \underline{n}(t) \\ \Rightarrow \mathbb{R}_{xx} &= \mathbb{H} \cdot \mathbb{R}_{mm} \cdot \mathbb{H}^H + \mathbb{R}_{nn} \end{aligned} \quad (2,14)$$

where,  $\mathbb{R}_{mm}$  is the covariance matrix of  $\underline{m}(t)$ .

In the absence of channel state information at the transmitter, it is reasonable to take the assumption that each antennas at the transmitter transmitting with the same power,  $\left(\frac{P_s}{M}\right)$  So assuming that the transmitted signal vector is composed of M statistically independent equal power  $\left(\frac{P_s}{M}\right)$  components with a gaussian distribution, the covariance matrix of the transmitted signal can be expressed as,

$$\mathbb{R}_{mm} = \frac{P_s}{M} \cdot \mathbb{I}_M \quad (2,15)$$

where,  $\mathbb{I}_M$  is M x M identity matrix.

The noise covariance matrix,  $\mathbb{R}_{nn}$ , of the complex N dimensional AWGN,  $n(t)$ , at the receiver with statistically independent power  $P_n$  in each of the N receiving antennas is,

$$\mathbb{R}_{nn} = P_n \cdot \mathbb{I}_N \quad (2,16)$$

where,  $\mathbb{I}_N$  is N x N identity matrix.

So the expression of the covariance matrix of the received signal becomes,

$$\begin{aligned} \mathbb{R}_{xx} &= \mathbb{H} \cdot \frac{P_s}{M} \cdot \mathbb{I}_M \cdot \mathbb{H}^H + P_n \cdot \mathbb{I}_N \\ &= \frac{P_s}{M} \cdot \mathbb{H} \cdot \mathbb{I}_M \cdot \mathbb{H}^H + P_n \cdot \mathbb{I}_N \end{aligned}$$

Putting the above expression of the covariance matrices in Eqn. 2.13, the expression of capacity becomes,

$$\begin{aligned}
C &= \frac{1}{2} \log_2 \frac{|\mathbb{R}_{xx}|}{|\mathbb{R}_{nn}|} \\
&= \frac{1}{2} \log_2 \left| \frac{\mathbb{R}_{xx}}{\mathbb{R}_{nn}} \right| \\
&= \frac{1}{2} \log_2 \left\{ \det \left( \frac{\mathbb{R}_{xx}}{\mathbb{R}_{nn}} \right) \right\} \\
&= \frac{1}{2} \log_2 \left\{ \det \left( \frac{\frac{P_s}{M} \cdot \mathbb{H} \cdot \mathbb{I}_M \cdot \mathbb{H}^H + P_n \cdot \mathbb{I}_N}{P_n \cdot \mathbb{I}_N} \right) \right\} \\
&= \frac{1}{2} \log_2 \left\{ \det \left( \mathbb{I}_N + \frac{\frac{P_s}{M} \cdot \mathbb{H} \cdot \mathbb{I}_M \cdot \mathbb{H}^H}{P_n \cdot \mathbb{I}_N} \right) \right\} \\
&= \frac{1}{2} \log_2 \left\{ \det \left( \mathbb{I}_N + \frac{P_s}{P_n \cdot M} \cdot \frac{\mathbb{H} \cdot \mathbb{I}_M \cdot \mathbb{H}^H}{\mathbb{I}_N} \right) \right\} \\
&= \frac{1}{2} \log_2 \left\{ \det \left( \mathbb{I}_N + \frac{SNR}{M} \cdot \frac{\mathbb{H} \cdot \mathbb{I}_M \cdot \mathbb{H}^H}{\mathbb{I}_N} \right) \right\} \\
&= \frac{1}{2} \log_2 \left\{ \det \left( \mathbb{I}_N + \frac{SNR}{M} \cdot \mathbb{H} \cdot \mathbb{H}^H \right) \right\}
\end{aligned}$$

So the expression for the capacity of a MIMO communication system, subjected to Rayleigh fading, for the above mentioned scenario and assumptions is,

$$C = \frac{1}{2} \log_2 \left\{ \det \left( \mathbb{I}_N + \frac{SNR}{M} \cdot \mathbb{H} \cdot \mathbb{H}^H \right) \right\} \quad (2.17)$$

# Chapter 3

## Impact of Antenna Array Geometry

### 3.1 Array of Antennas

An array system is a collection of antennas which are spatially distributed at judicious locations in the 3-dimensional real space, with a common reference point [6]. The signals received by the array elements contain both temporal and spatial information about the array signal environment. This environment is usually contaminated by background and sensor noise. The main aim of array processing is to extract and then exploit this spatio-temporal information to the fullest extent possible in order to provide estimates of the parameters of interest (i.e. number of incident signals, Directions-of-Arrival (DOAs), Times-of-Arrival (TOAs), ranges, velocities etc) of the array signal environment.

The performance of array systems, especially the ones with super-resolution capabilities is, in general, limited by three main factors:

- a. The presence of inherent background and sensor noise.
- b. The limited amount of information the antennas can measure due to finite observation interval (number of snapshots) and array geometry.

- c. The lack of calibration, modeling errors and system uncertainties that are embedded in the received array signal-vector  $x(t)$ , which are not accounted for.

However, the overall quality of the system's performance is naturally a function of the array structure in conjunction with the geometrical characteristics of the signal environment, as well as algorithms employed.

### **3.2 Concept of Manifold Vector**

For a general non-linear array of sensors, the locus of manifold vectors is a hyperspace embaded in a multidimensional complex space, with azimuth and elevation angles as the parameter of interest [20]. To find the expression of manifold vector, let us consider an array of  $N$  sensors, with sensor locations,  $r$ , operating in the presence of  $M$  narrowband point sources and having the same known carrier frequency  $F_c$ . The modeling of the signal due to  $i$ -th emitter, received at the zero-phase reference point (taken to be the origin of the coordinate system) is determined by whether the source is located in, or close to, the array's near-field or in the array's far-field.

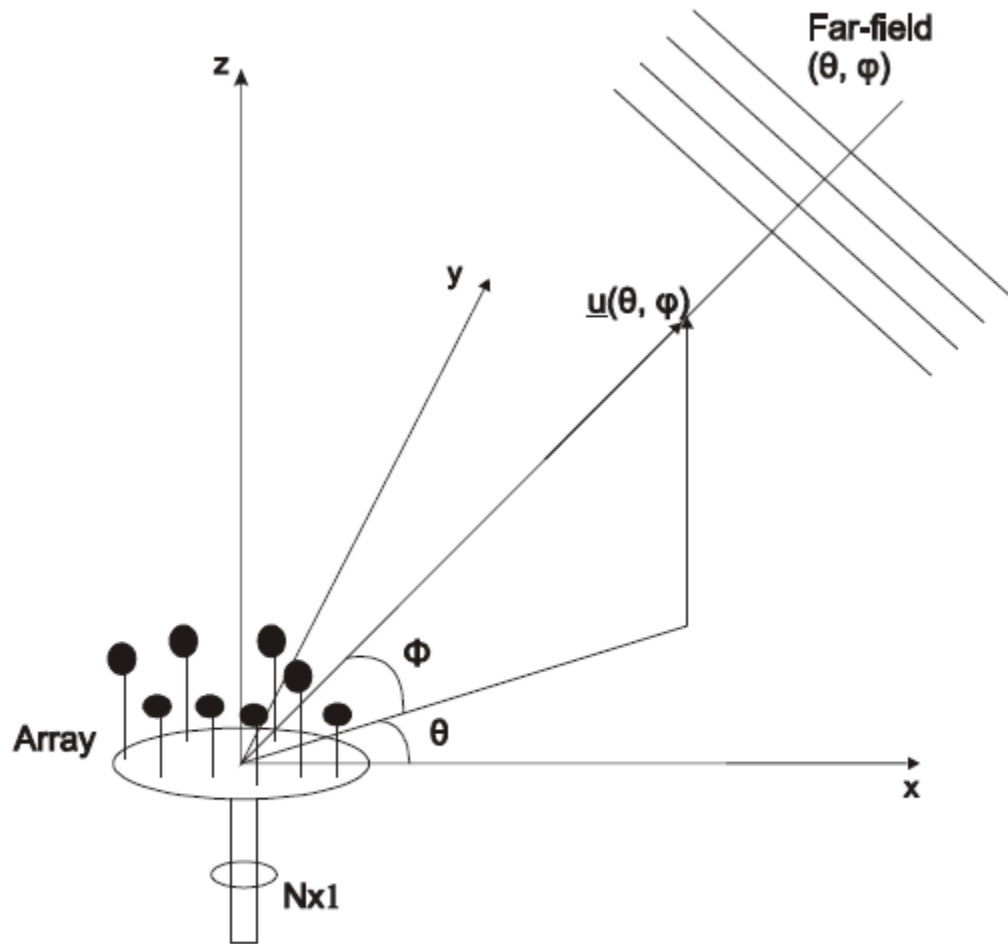


Figure 3.1: Relative Geometry between a far-field emitting source and an array of sensors

Whether the source is in near field or far field, is determined by the value of its range  $p_i$  with respect to the array aperture  $l_a$ . The aperture of the array is defined as,

$$l_a = \max_{\forall i,j} \left\| \underline{r}_i - \underline{r}_j \right\| \quad (3,1)$$

The region is determined according to the following conditions,

- a. Near-field or Fresnel zone: if  $\rho_i \approx \frac{2l_a}{\lambda}$
- b. Far-field or Fraunhofer zone: if  $\rho_i \gg \frac{2l_a}{\lambda}$
- c. Near far field: if  $\rho_i > \frac{2l_a}{\lambda}$  but not  $\rho_i \gg \frac{2l_a}{\lambda}$

Where  $\lambda$  is the wavelength of the transmitted signal.

For Near-field and Near far field, the spherical wave propagation model is used and for Far-field plane wave propagation is assumed.

Based on the above discussion and by considering the M sources in the Near-field of the array, the array signal is the superposition of the spherical waves from each individual source.

The signal from the  $i$ th emitter in accordance with Figure 3.2, received at the zero-phase reference point is,

$$\begin{aligned}
 & \sqrt{P} \cdot m_i\left(t - \frac{\rho_c}{c}\right) \exp(j2\Pi F_c t) \cdot \frac{1}{\rho_o} \exp(j2\Pi F_c \frac{\rho_o}{c}) \\
 \approx & \sqrt{P} \cdot m_i(t) \exp(j2\Pi F_c t) \cdot \frac{1}{\rho_o} \exp(j2\Pi F_c \frac{\rho_o}{c}) \\
 \Rightarrow & \sqrt{P} \cdot m_i(t) \exp(j2\Pi F_c t) \cdot \beta \\
 \Rightarrow & \sqrt{P} \cdot \beta \cdot m_i(t) \exp(j2\Pi F_c t)
 \end{aligned}$$

where,

$m_i(t)$  complex envelop of the transmitted signal

P is the power of the transmitted signal

$\exp(j2\Pi F_c t)$  carrier used at the transmitter.

$\rho_o$  distance of the zero-phase reference point from the ith emitter

$\beta = \frac{1}{\rho_o} \exp(j2\Pi F_c \frac{\rho_o}{c})$  fading coefficient of the transmission link

The signal arriving at the kth sensor will be a delayed version of the signal received at the zero-phase reference point. So the signal, after traveling some additional distance, arriving at the kth sensor,

$$\begin{aligned} & \sqrt{P}.m_i(t) \exp(j2\Pi F_c t) \cdot \frac{1}{\rho_k} \exp(-j2\Pi F_c \frac{\rho_k}{c}) \\ \Rightarrow & \sqrt{P}.m_i(t) \exp(j2\Pi F_c t) \cdot \frac{\rho_o}{\rho_k} \cdot \frac{1}{\rho_o} \exp(-j2\Pi F_c \frac{\rho_o + l}{c}) \\ \Rightarrow & \sqrt{P}.m_i(t) \exp(j2\Pi F_c t) \cdot \frac{1}{\rho_o} \exp(-j2\Pi F_c \frac{\rho_o}{c}) \cdot \frac{\rho_o}{\rho_k} \exp(-j2\Pi F_c \frac{l}{c}) \\ \Rightarrow & \sqrt{P}.\beta.m_i(t) \exp(j2\Pi F_c t) \cdot \frac{\rho_o}{\rho_k} \exp(-j2\Pi F_c \frac{l}{c}) \end{aligned}$$

where,

$\rho_k$  distance of the kth sensor from the ith emitter

$l$  extra distance the signal has to travel to reach the kth sensor

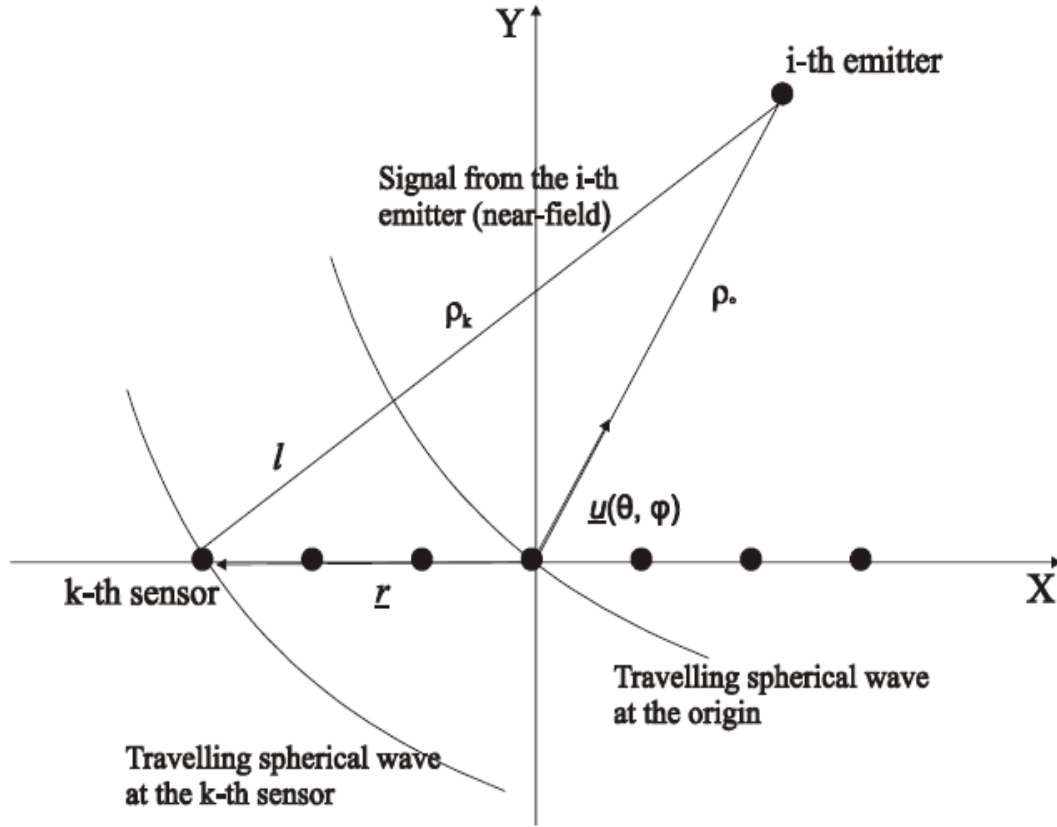


Figure 3.2: Geometry of travelling spherical wave, relative to the k-th sensor and the array reference point

This extra distance can be expressed as a function of the DoA of the  $i$ th signal and the position of the  $k$ th sensor with respect to the zero-phase reference point. So the expression of the extra distance,  $l$ , the signal has to travel to reach the  $k$ th sensor is,

$$\begin{aligned}
 l &= \rho_k - \rho_o \\
 &= \|\underline{r} - \rho_o \underline{u}(\theta, \phi)\| - \rho_o \\
 &= \sqrt{(\underline{r} - \rho_o \underline{u}(\theta, \phi))^T (\underline{r} - \rho_o \underline{u}(\theta, \phi))} - \rho_o \\
 &= \sqrt{\underline{r}^T \underline{r} - 2\rho_o \underline{u}(\theta, \phi)^T \underline{r} + \rho_o^2} - \rho_o
 \end{aligned}$$

So, the path difference introduced as a result of array geometry is,

$$l = \sqrt{\underline{r}^T \cdot \underline{r} - 2\rho_o \cdot \underline{u}(\theta, \phi)^T \cdot \underline{r} + \rho_o^2} - \rho_o \quad (3,2)$$

where,

$$\underline{r} = [r_x, r_y, 0]^T$$

$r_x$  is the x coordinate of the  $i$ th emitter

$r_y$  is the y coordinate of the  $i$ th emitter

$$\underline{u}(\theta, \phi) = \begin{bmatrix} \cos \theta \cdot \cos \phi & \sin \theta \cdot \cos \phi & \sin \phi \end{bmatrix}^T$$

$\theta$  is the azimuth angle, measured anticlockwise from the positive x-axis

$\phi$  is the elevation angle, measured anticlockwise from the positive x – y plane

So using the expression of Eqn. 3.2, the signal arriving from the  $i$ th emitter, received at the  $k$ th sensor is,

$$\begin{aligned} & \sqrt{P} \cdot \beta \cdot m_i(t) \exp(j2\Pi F_c t) \cdot \frac{\rho_o}{\sqrt{\underline{r}^T \cdot \underline{r} - 2\rho_o \cdot \underline{u}(\theta, \phi)^T \cdot \underline{r} + \rho_o^2}} \\ & \cdot \exp(-j2\Pi \frac{F_c}{c} (\sqrt{\underline{r}^T \cdot \underline{r} - 2\rho_o \cdot \underline{u}(\theta, \phi)^T \cdot \underline{r} + \rho_o^2} - \rho_o)) \end{aligned}$$

Defining the 'array manifold vector'.  $S$ , as

$$\underline{S} = \frac{\rho_o}{\sqrt{\underline{r}^T \cdot \underline{r} - 2\rho_o \cdot \underline{u}(\theta, \phi)^T \cdot \underline{r} + \rho_o^2}} \exp(-j2\Pi \frac{F_c}{c} (\sqrt{\underline{r}^T \cdot \underline{r} - 2\rho_o \cdot \underline{u}(\theta, \phi)^T \cdot \underline{r} + \rho_o^2} - \rho_o)) \quad (3,3)$$

When measure in the units of half wavelengths, the expression of .array manifold vector becomes,

$$\underline{S} = \frac{\rho_o}{\sqrt{\underline{r}^T \underline{r} - 2\rho_o \underline{u}(\theta, \phi)^T \underline{r} + \rho_o^2}} \exp(-j2\Pi(\sqrt{\underline{r}^T \underline{r} - 2\rho_o \underline{u}(\theta, \phi)^T \underline{r} + \rho_o^2} - \rho_o)) \quad (3,4)$$

The expression of the signal arriving from the ith emitter, received at the kth sensor becomes,

$$\sqrt{P} \cdot \beta \cdot m_i(t) \exp(j2\Pi F_c t) \cdot \underline{S}$$

When the source is in the Far-field region of the receiver, then the expression of the 'array manifold vector' reduces to,

$$\underline{S} = \exp(-j2\Pi \underline{r}^T \cdot \underline{u}(\theta, \phi)^T) \quad (3.5)$$

### 3.3 Impact of Manifold Vector on System Capacity

#### 3.3.1 Impact of Manifold Vector

In this section the results of using manifold vector for multiple source detection problems is presented. The scenario is as described bellow, Uniform linear array (ULA) is used in both transmitter and receiver as shown in Figure fg3.3. In the transmitting end an ULA of 3 elements is positioned at an angle of 30 degree with the horizontal axis and an ULA of 5 elements is placed at the receiving end at an angle of 15 degree with the horizontal axis. The transmitter and receiver

array are placed  $1000\lambda/2$  units apart at an angle of 70 degree with the horizontal axis. The inter-element spacing for both transmitter and receiver array is  $\lambda/2$ .

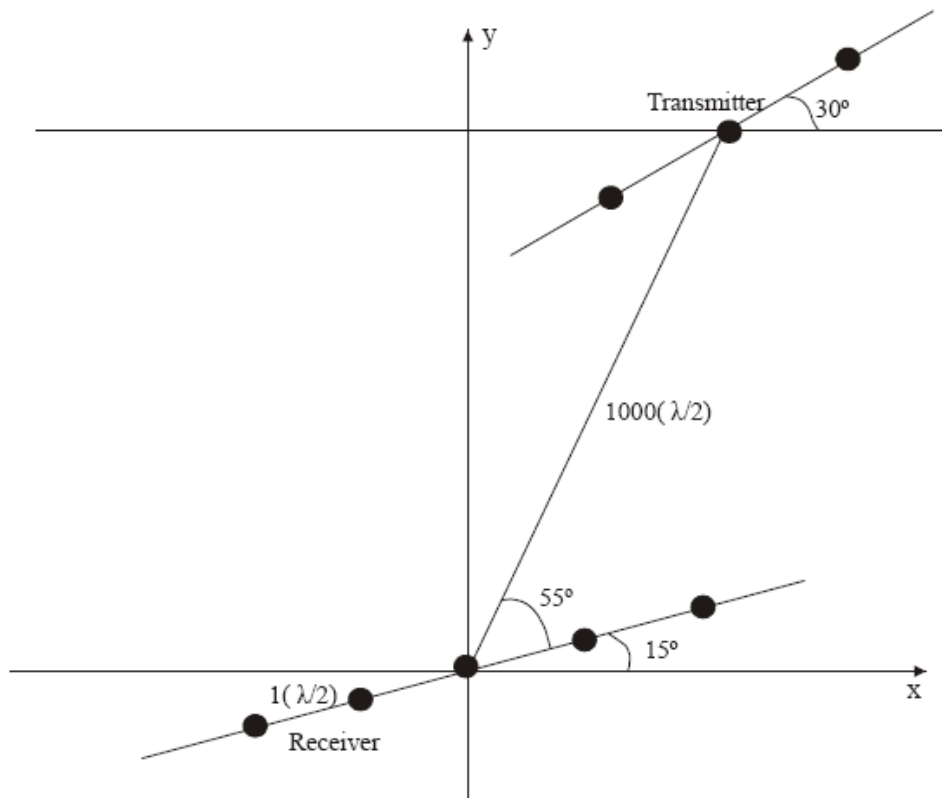


Figure 3.3: Scenario for multiple source detection with MIMO system

### 3.3.2 Channel Matrix Considering Antenna Array Geometry

Expression of the channel matrix is derived from the expression of received signal for SISO system. This expression of the channel matrix will be used in the expression of capacity to consider the impact antenna array geometry exerts.

#### ii. SISO channel model:

The channel model for single input vector output (SISO) channel is given in Figure 3.6. The received signal at the output of the receiver antenna array,

considering the affect of k multipath, can be modeled in accordance with the figure as,

$$\begin{aligned}
 \underline{x}(t) &= \sum_{j=1}^k m_j(t) \cdot \underline{\beta}_j \circ \underline{S}^{Rx} + \underline{n}(t) \\
 &= \sum_{j=1}^k \underline{\beta}_j \circ \underline{S}^{Rx} \cdot m_j(t) + \underline{n}(t) \\
 &= \sum_{j=1}^k \underline{H}_j \cdot m(t)_j + \underline{n}(t)
 \end{aligned}$$

So the received signal at the output of the array is,

$$\underline{x}(t) = \sum_{j=1}^k \underline{H}_j \cdot m(t)_j + \underline{n}(t) \tag{3.6}$$

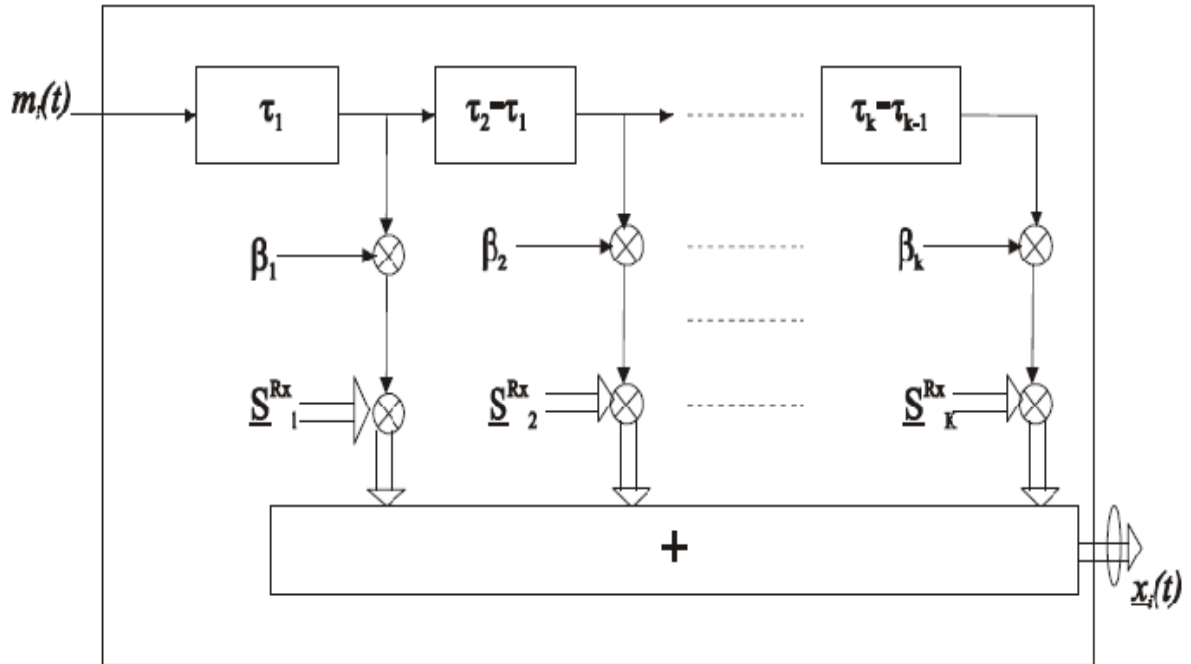


Figure 3.4 SISO Channel Model

where,

Channel Matrix,

$$H_i = \underline{\beta}_j \underline{S}^{Rx}$$

### 3.4 Expression of Capacity Considering Array Geometry

The expression of capacity of a MIMO communication derived in the previous chapter ( Eqn. 2.17 ) is again given here for convenience,

$$C = \frac{1}{2} \log_2 \left\{ \det \left( \mathbb{I}_N + \frac{SNR}{M} \cdot \mathbb{H} \cdot \mathbb{H}^H \right) \right\}$$

When the channel matrix comprises fading coefficient and both the transmitter and receiver array geometry, the overall channel matrix of a MIMO system can be expressed as in the previous section,

$$\mathbb{H} = (\underline{S}^{Rx} \cdot \underline{S}^{TxH}) \circ \mathbb{B} \quad (3.7)$$

Substituting the value of the overall channel matrix in Eqn. 2.17, we have the expression of the capacity of a MIMO communication system as a function of the antenna array geometry of the receiver and the transmitter. The expression of the capacity becomes,

$$C = \frac{1}{2} \log_2 \left\{ \det \left( \mathbb{I}_N + \frac{SNR}{M} \cdot ((\underline{S}^{Rx} \cdot \underline{S}^{TxH}) \circ \mathbb{B}) \cdot ((\underline{S}^{Rx} \cdot \underline{S}^{TxH}) \circ \mathbb{B})^H \right) \right\} \quad (3.8)$$

## Chapter 4

### Simulation Results

Throughout this thesis, the entire focus was given on the impact geometry of antenna array, both on transmitter and receiver, has on the capacity of MIMO communication system. Different antenna geometries are being used in transmitter and receiver. Uniform Linear Array (ULA), Non-Uniform Linear Array (NULA), Circular Array (CA), Star Array (StA), Hexagonal Array (HA) and Square Array (SA) geometries are being tried to observe the impact of array geometry on system capacity. Throughout the simulations, specific scenario is being assumed, which will be described in the next section. First the simulation was

conducted without using beamforming technology. Comments on the simulation and motivation to go for beamforming technology are given on the comments section. Different aspects of the antenna geometry and channel environment are being varied and the impact of the change on the system capacity is observed. The following aspects of the antenna array geometry and communication environment were of main interest,

- a. Signal to Noise Ratio (SNR)
- b. Angle of Arrival of the Received Signal
- c. Antenna Array Configuration
- d. Number of Element in the Antenna Array
- e. Inter-element Spacing in the Antenna Array

In the next section the general scenario for all the simulations will be described. All the simulation results obtained varying the above aspects with and without employing beamforming technique will be given in section 4.2, 4.3 and 4.4 and comments will be given for the results obtained.

#### **4.1 General Scenario for the Simulations**

For the simulations to observe the impact of antenna geometry on system capacity, the following scenario is being assumed throughout. Both transmitter and receiver are using antenna array. When SIVO system is used, it will be mentioned specifically. Transmitter and receiver are positioned 1000 unit (in half wavelength) apart. The inter-element spacing for the antenna arrays is 1 unit (in half wavelength). The reference point of the receiver antenna array is taken to be at the origin of the co-ordinate system. Number of elements in the antenna array is taken to be seven unless otherwise mentioned. Antenna array geometry will be mentioned along specific simulations. Narrow band channel is assumed which is subjected to Rayleigh fading. The environment is assumed to have sufficient

number of scatterers so as to provide rich scattering to justify the Rayleigh fading assumption. Noise received at the receiver is assumed to be additive white gaussian with zero mean and unit variance. The scenario is depicted in Figure 4.1 for uniform linear array (ULA) of seven elements at both transmitter and receiver.

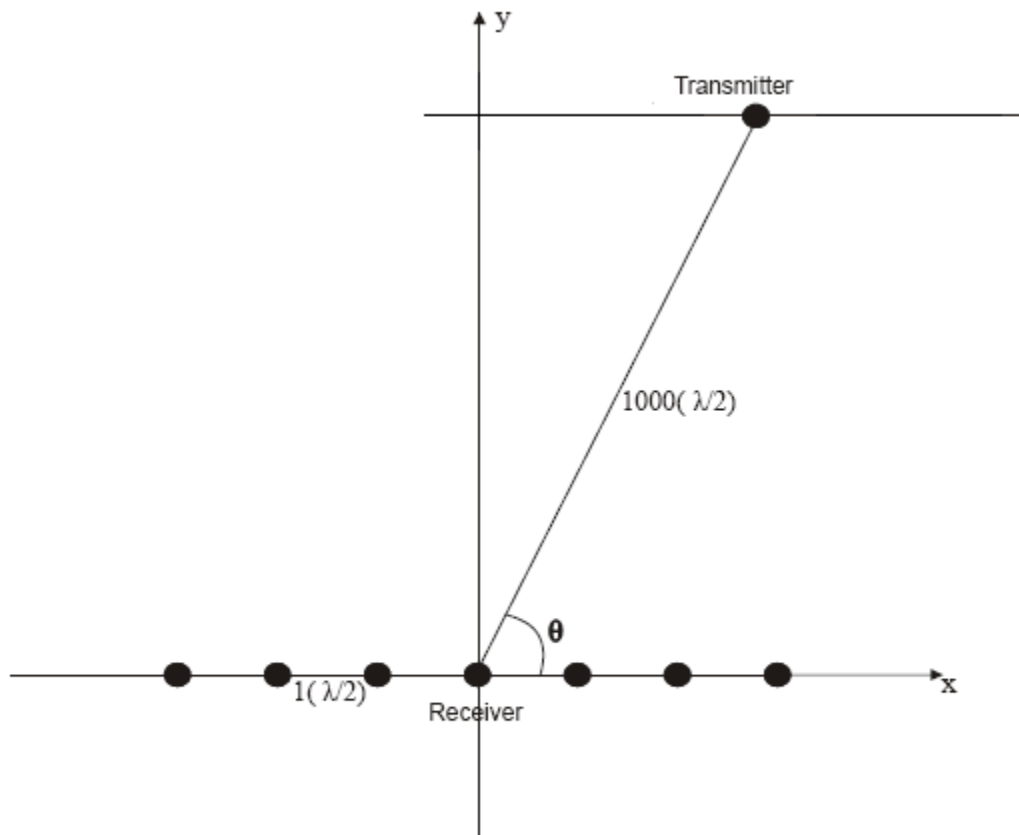


Figure 4.1: General Scenario for Simulations

#### 4.2 SIVO System Without Using Beamforming Techniques

In this section the results of the observations of the impact of antenna geometry on the capacity of the SIVO system without using beamforming technique are

given. Number of elements at the transmitter is one and that at the receiver is seven. The signal is arriving at the receiver at an angle of  $70^\circ$ .

#### 4.2.1 Impact of SNR and Angle of Arrival (AoA) on Capacity

In this section results for the simulations to investigate the influence of changing SNR and AoA on the system capacity is provided. Figure 5.2 gives the comparison about the impact different antenna array geometry has on the system capacity.

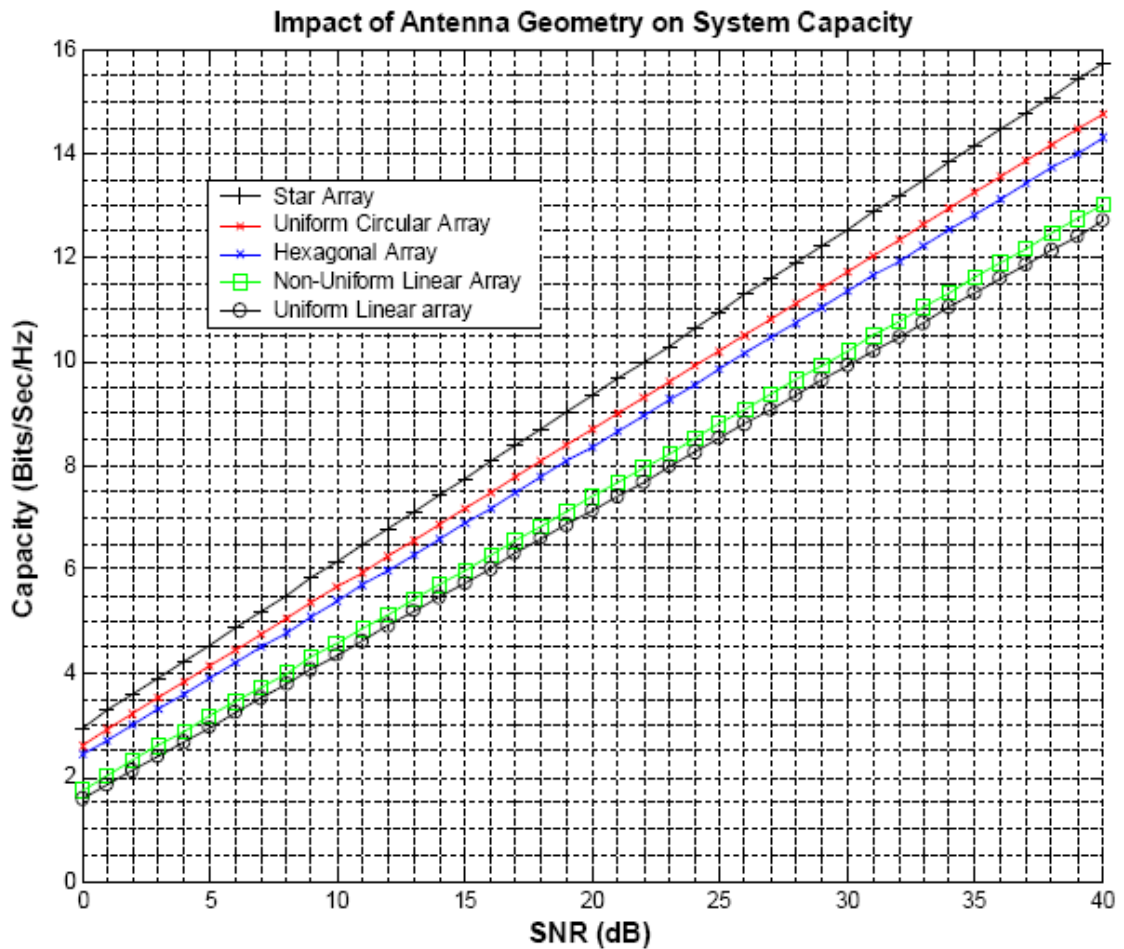


Figure 4.2: Impact of Different Antenna Geometry on Capacity For SIVO systems

It is found that for an angle of arrival of  $70^\circ$ , Star Array outperforms the other four configurations. The impact of using different antenna array geometries is not that significant in this case. All of the configurations used produced almost similar results. The capacity of the system using different array geometries seems to have almost a linear relationship with SNR. As shown in Figure 5.2, Star array configurations yields the best result compared to the other configurations used. The capacity of ULA drops down due to the high spatial correlation. NULA provides slightly better capacity than ULA. The Hexagonal Array yields slightly lower capacity than UCA because of its compact geometry. Next both SNR and AoA were varied for different antenna geometry and the results were observed. Figure 4.3 - 4.7 depicts the change in capacity as we change SNR and AoA for Uniform Linear Array (ULA), Non-Uniform Linear Array (NULA), Uniform Circular Array (UCA), Hexagonal Array (HA) and Star Array (StA) respectively. SNR was varied from 0 dB to 40 dB and angle of arrival ranging from 0 to 180 deg were tried.

Impact of SNR and AoA on Capacity using Uniform Linear Array

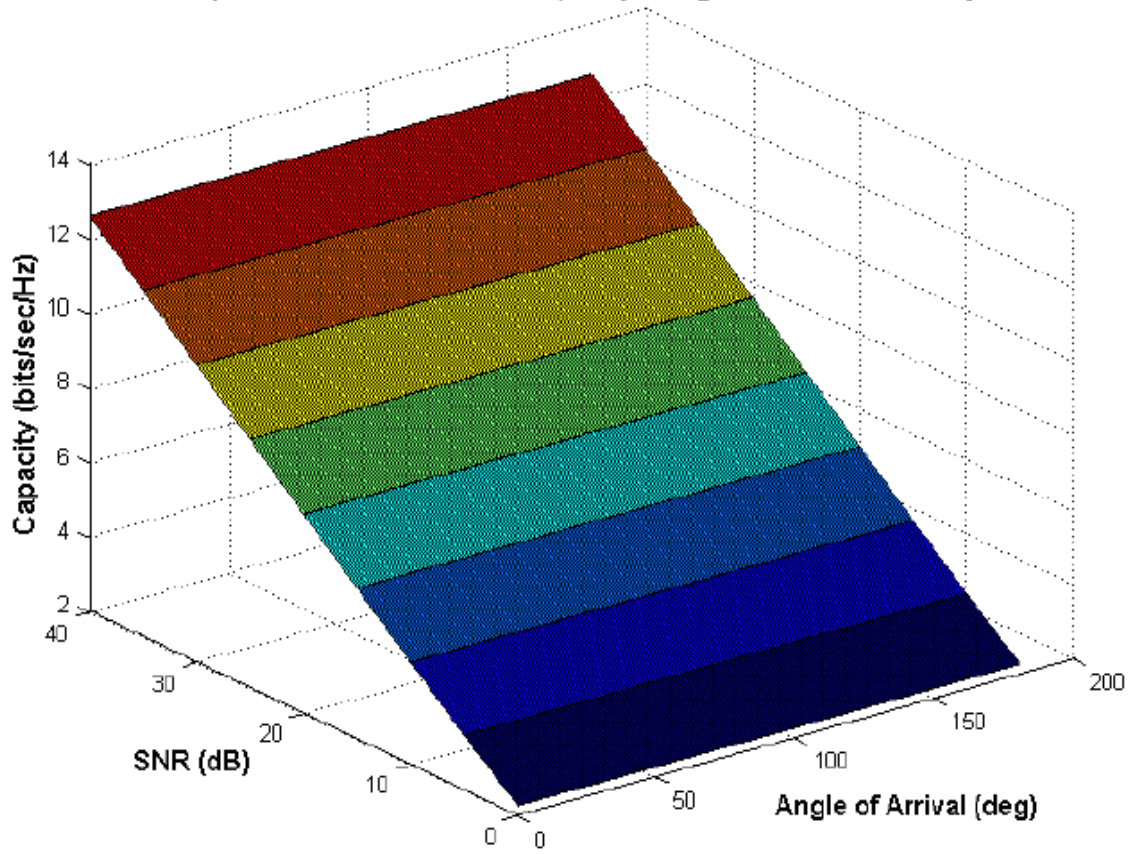
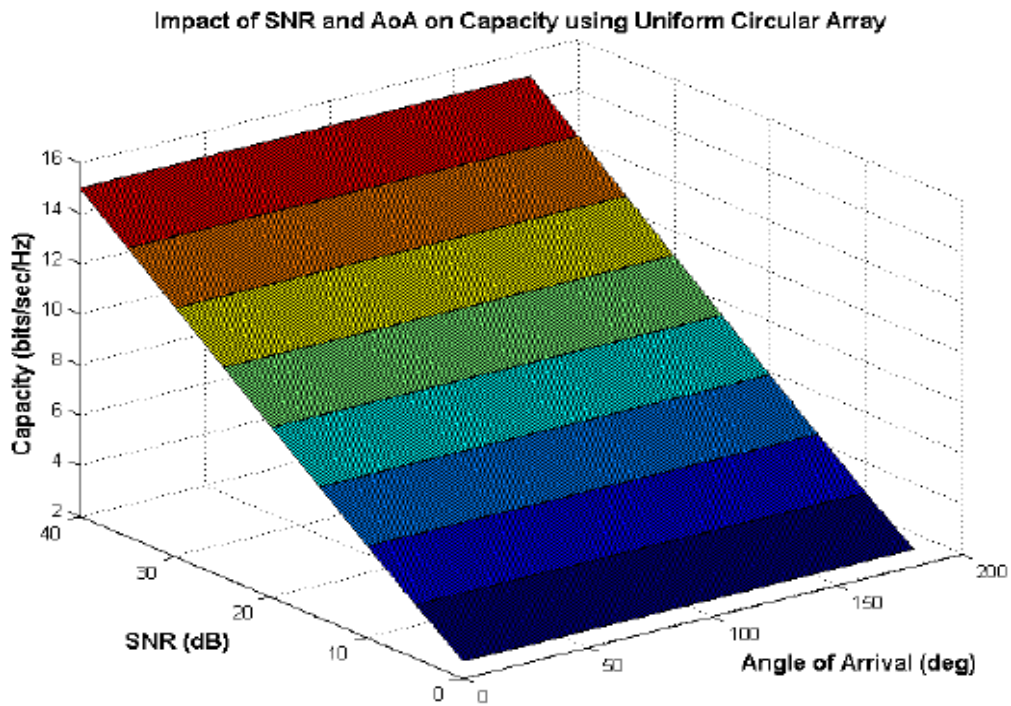
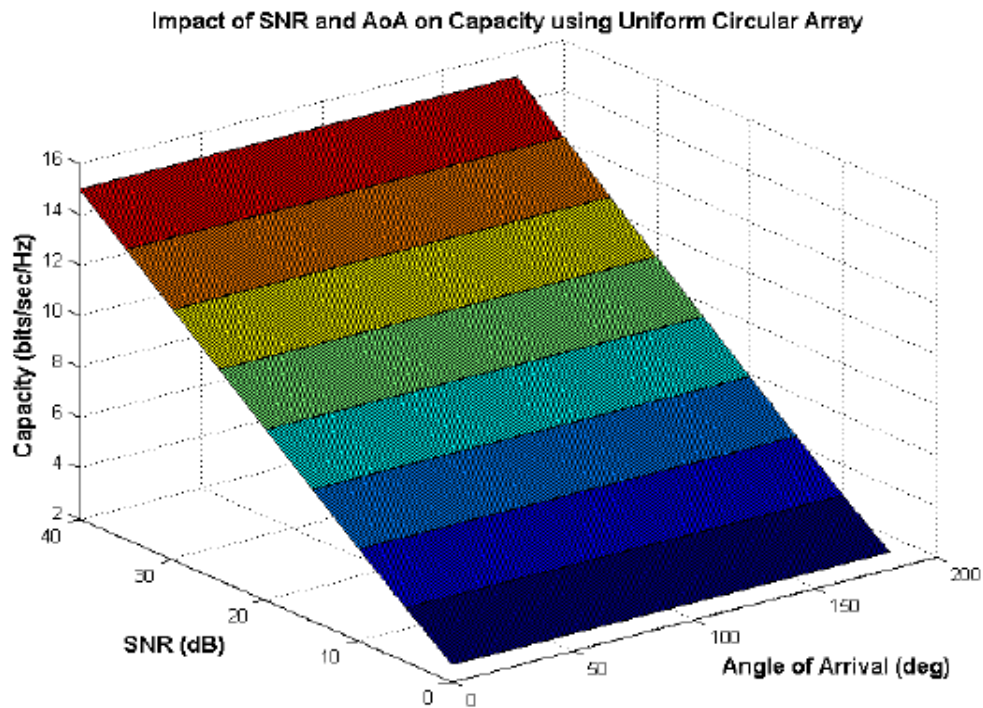


Figure 4.3: Variation in System Capacity Using Uniform Linear Array



**Figure 4.4: Variation in System Capacity Using Non-Uniform Linear Array**



**Figure 4.5: Variation in System Capacity Using Uniform Circular Array**

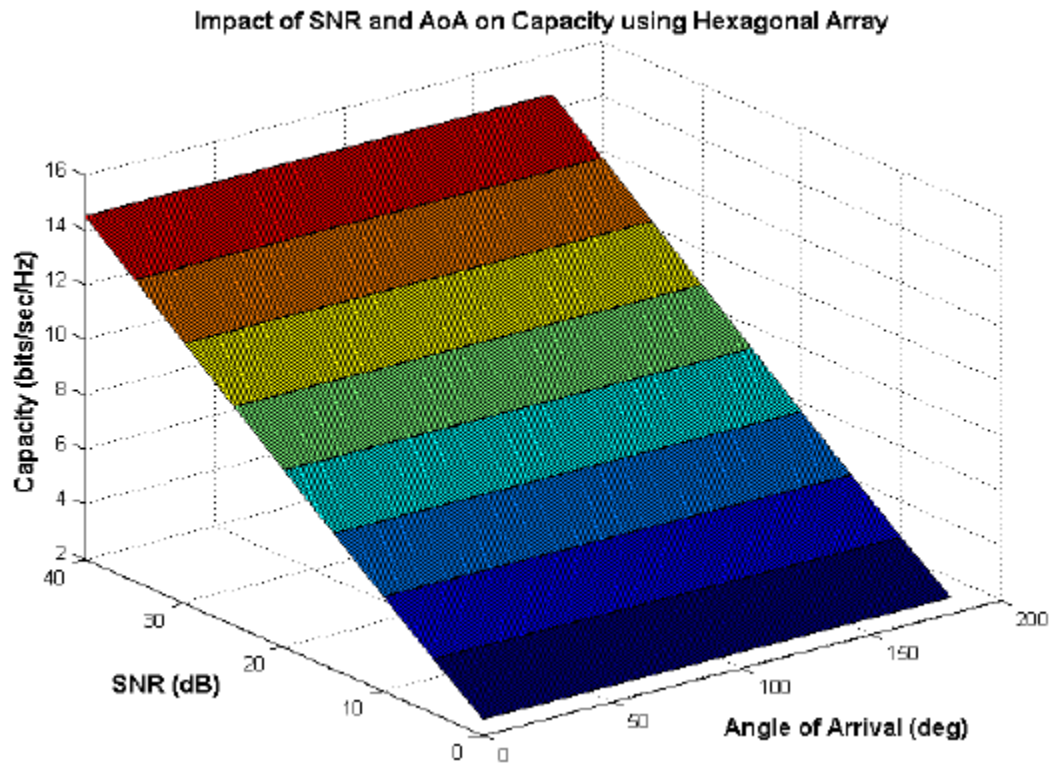


**Figure 4.6: Variation in System Capacity Using Hexagonal Array**

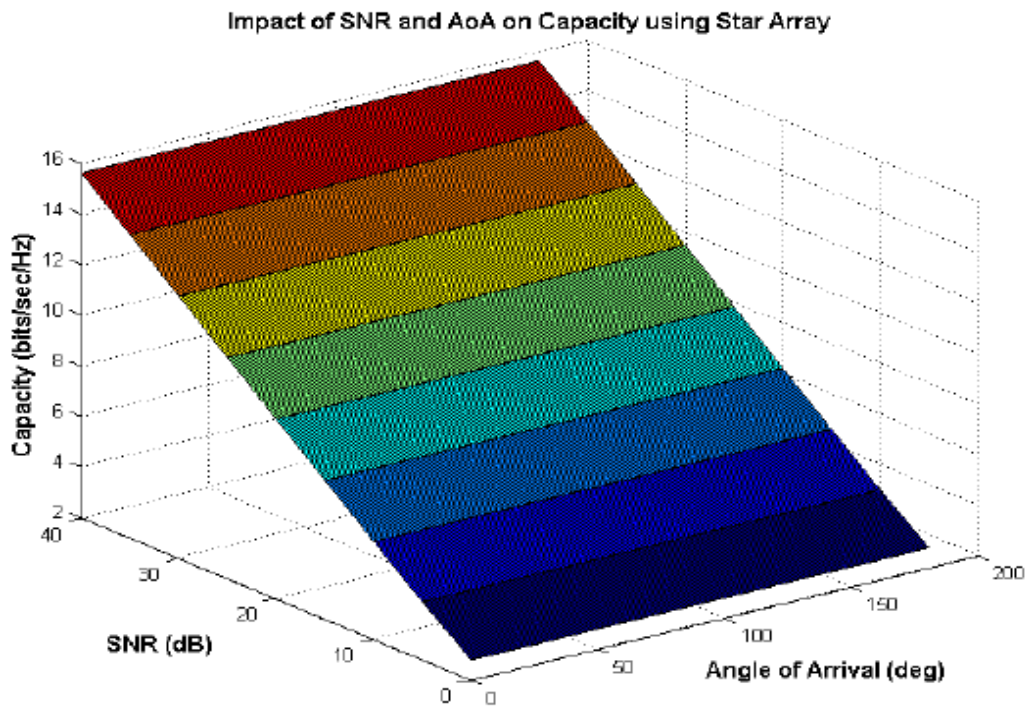


**Figure 4.7: Variation in System Capacity Using Star Array**

### 4.2.2 Impact of Number of Array Elements on Capacity

In this section number of antenna array elements was varied for array configuration of ULA. ULA with 7,6,5,4 and 3 elements were used at the receiver keeping the inter-element spacing fixed at half wavelength. As expected the value of capacity increased as number of elements of antenna array was increased. Figure 5.8 plots capacity as a function of SNR for different number of array elements.

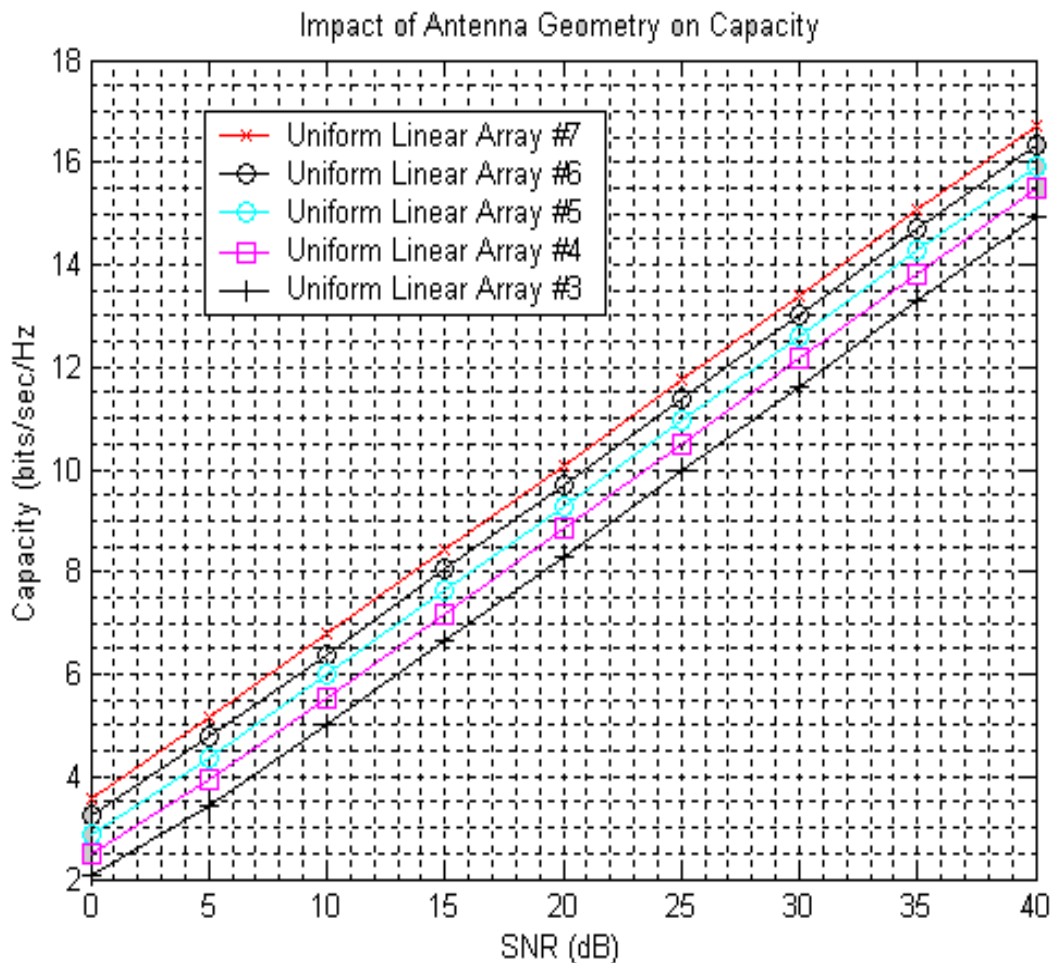
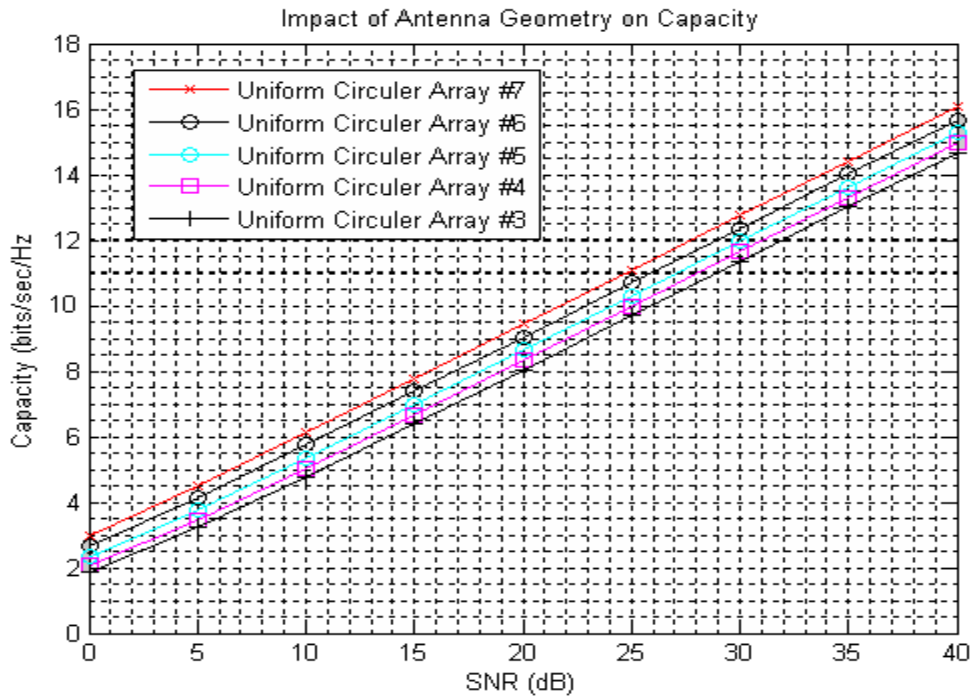
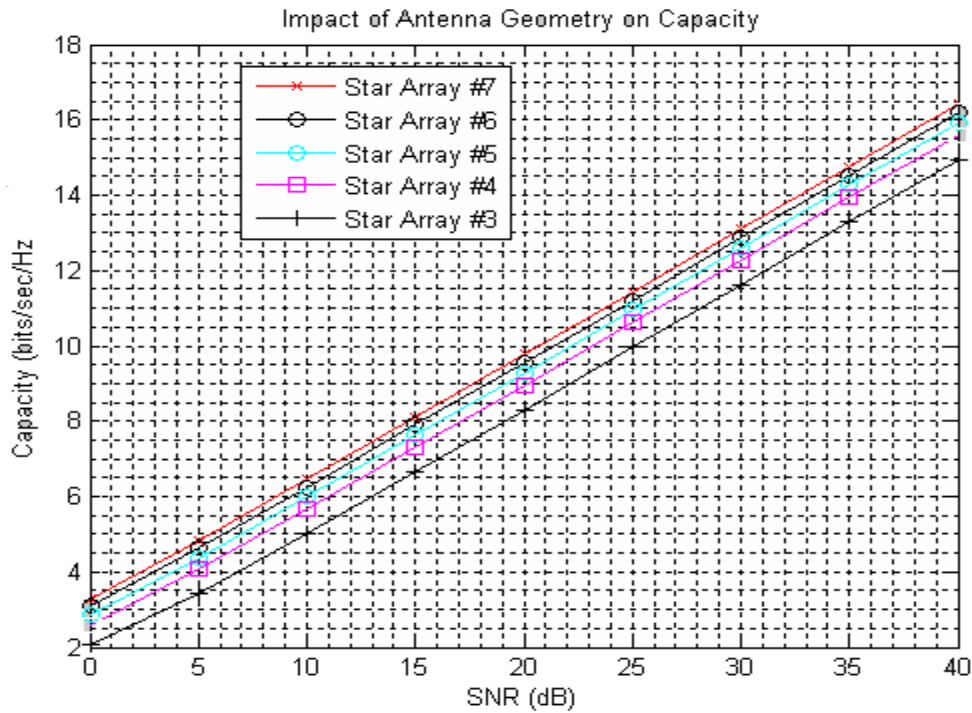


Figure 4.8: Change in Capacity with change in Number of Array Elements for Uniform Linear Array



**Figure 4.9: Change in Capacity with change in Number of Array Elements for Uniform Circular Array**



**Figure 4.10: Change in Capacity with change in Number of Array Elements for Star Array**

### **4.2.3 Comments on Simulation Results**

For SIVO system the impact of SNR and AoA for different antenna geometry on the capacity is observed in this section. No beamforming technique were employed to estimate the value of capacity. It was found that capacity increases with SNR and number of elements in the array. But when AoA of the received signal was varied, there was no change in the value of the capacity, which is unexpected. As can be seen in Figure 4.3 - 4.7, five different antenna array configurations produced same result. No change in the value of capacity was observed when the AoA was varied from 0 deg to 180 deg. This may be the result of not using any beamforming technique either at the receiver or at the transmitter. For this reason the value of capacity are just the averaged value, whatever the value of the AoA of the received signal is, and same for all AoAs. If the receiver has some information about the approximate location of its desired source, then this information can be used to give higher weight to the signal coming from that particular direction.

## **Chapter 5**

### **Conclusions and Future Works**

This report provides a brief overview of the impact antenna array geometry has on the capacity of the system. Five different array configurations, Uniform Linear Array, Non-Uniform Linear Array, Uniform Circular Array, Hexagonal Array and Star Array, were used to analyze the influence their geometries have on the capacity.

At first we compare the system capacity for these five array configurations with the change of SNR. The system capacity seems to have almost linear relationship with SNR. We find that Star Array gives best result among all the configurations. While the system capacity using Uniform Linear Array drops down. We also observe the impact of system capacity by varying both SNR and AoA. There was no significant change in the magnitude of system capacity for the change of AoA. Because we have used SISO system without beamforming technique. In SISO system if we use beamforming technique at the receiver there will be change in the system capacity with the change of AoA.

As was expected, the capacity increased as number of elements in the array was increased. Compared to the baseline case (SISO system), which by Shannon's classical formula scales as one more bits/cycle for each 3 dB of SNR increase, remarkably with MIMO, the scaling is almost like  $n$  more bits/cycle for each 3 dB increase in SNR. But in this case the inter-element spacing was kept fixed. So increasing number of element consequently resulted in increased antenna aperture and increased antenna size. For practical limitations, the size of the array is limited to a certain limit. So achieving a significant amount of capacity keeping inter-element spacing fixed is not realistic.

We can achieve significant improvement in system capacity using antenna array at both the transmitter and receiver. When antenna array is used at both end of the transmission link, it increases the spatial dimensions, which allows the use of subspace techniques and other processing. So the capacity of the system increases significantly with MIMO system compared to that achievable with SISO systems.

In this report it was assumed that the receiver has the perfect information about the channel and the transmitter doesn't have any information about the channel. The analysis is conducted in an idealized context for a quasi-static channel that

is subject to Rayleigh fading. But in real life these assumptions are not always satisfied as the channel sometimes changes frequently with time, violating the quasi-static channel assumption. New schemes of increasing the number of array elements without reducing inter-element spacing (or without increasing spatial correlation) certainly going to improve the system capacity significantly. The combination of space-time coding, efficient array configuration, accurate tracking of the transmission link and perfect knowledge about the channel at both transmitter and receiver would require much more research. MIMO communication system certainly is significant and visionary step forward towards next generation communications.

# Bibliography

- [1] C. E. Shannon, .A Mathematical Theory of Communication., Reprinted with correction from the Bell System Technical Journal, Vol. 27, pp. 379-423, 623-656, July, October, 1948.
- [2] G. J. Foschini and M. J. Gans, .On Limits of Wireless Communications in a Fading Environment when Using Multiple Antennas., Wireless Personal Communications, Vol. 6, pp. 311-335, 1998.
- [3] G. J. Foschini and M. J. Gans, .Layered Space-Time Architecture for Wireless Communication in a Fading Environment when Using Multi-Element Antennas., Bell Labs Tech. J., Vol. 1, pp. 41-59, 1996.
- [4] I. E. Telatar, .Capacity of Multi-antenna Gaussian Channels., European Transactions on Telecommunications, Vol. 10, no. 6, pp. 585-595, Nov./Dec., 1995.
- [5] A. J. Paulraj, D. A. Gore, R. U. Nabar, H. Bolcskei, "An Overview of MIMO Communications .A Key to Gigabit Wireless., Proceeding of the IEEE, Vol. 92, no. 2, Feb., 2004.
- [6] A. Manikas, Differential Geometry in Array Processing, Imperial College Press, 57 Shelton Street, Covent Garden, London WC2H 9HE.
- [7] A. J. Paulraj, R. U. Nabar, D.A. Gore, Introduction to Space-Time Wireless Communications, Cambridge University Press, 40 West 20th Street, New York, USA, 2003.
- [8] T. M. Cover, J. a. Thomas, Elements of Information Theory, Wiley Series in Telecommunications, Wiley-Interscience Publication.
- [9] A. Forenza, R. W. Heath Jr., .Impact of Antenna Geometry on MIMO Communication in Indoor Clustered Channels., Antennas and Propagation Society Symposium, 2004. IEEE, Vol. 2, 20-25, June 2004, pp. 1700-1003.
- [10] R.B. Ertel, P. Cardieri, K.W. Sowerby, T.S. Rappaport, J.H. Reed, .Overview of spatial channel models for antenna array communication systems., Personal Communications, IEEE [see also IEEE Wireless Communications], Volume 5, Issue 1, Feb. 1998 Page(s):10 .22
- [11] A. Saleh, R. Valenzuela, .A Statistical Model for Indoor Multipath Propagation., Selected Areas in Communications, IEEE Journal, Vol. 5, Issue 2, Feb. 1987, Page(s): 128-137

- [12] Q.H. Spencer, A.L. Swindlehurst, .Some results on channel capacity when using multiple antennas., Vehicular Technology Conference, 2000. IEEE VTS-Fall VTC 2000. 52nd Volume 2, 24-28 Sept. 2000 Page(s):681 - 688 vol.2
- [13] M.A. Khalighi, J.M. Brossier, G.V. Jourdain, K. Raoof, .Water .lling capacity of Rayleigh MIMO channels., Personal, Indoor and Mobile Radio Communications, 2001 12th IEEE International Symposium, Volume 1, 30 Sept.-3 Oct. 2001 Page(s):A-155 - A-158 vol.1
- [14] J. Winters, "On the capacity of radio communication systems with diversity in a Rayleigh fading environment", IEEE J. Sel. Areas Commun., vol. 5, pp. 871-878, June 1987.
- [15] R. Farrukh, "Investigation of Arrayed MIMO System", Report (Msc and DIC), Department of Electrical and Electronic Engineering, Imperical College, London, 2004.
- [16] A. Manikas, "Lecture Notes: Advanced Communication Theory", Department of Electrical and Electronic Engineering, Imperial College, London, 2004-2005.
- [17] S. A. Jafar, "Fundamental Capacity Limits of Multiple Antenna Wireless Systems", PhD dissertation, Department of Electrical Engineering, Stanford University, 2003.
- [18] R. Galager, Information Theory and Reliable Communication, John Wiley and Sons, Inc., 1968.
- [19] A. Goldsmith, S. A. Jafar, N. Jindal and S. Vishwanath, .Capacity Limits of MIMO Channels., IEEE journal on selected areas in communications, VOL. 21, No. 5, June 2003.
- [20] A. Sleiman, A. Manikas, .Antenna Array Manifold: A Simplified Representation. IEEE Proceedings of ICASSP, Vol.5, pp.3164-3167, June 2000.
- [21] G. J. Foschini, "Layered space-time architecture for wireless communication in a fading environment when using multiple antennas," *Bell Labs Technical Journal*, vol. 1, no. 2, pp. 41–59, 1996.
- [22] A. Paulraj and T. Kailath, "U. S. #5345599: Increasing capacity in wireless broadcast systems using distributed transmission/directional reception (DTDR)," Sept. 1994.

- [23] R. J. Piechocki, P. N. Fletcher, A. R. Nix, C. N. Canagarajah, and J. P. McGeehan, "Performance evaluation of BLAST-OFDM enhanced hiperlan/2 using simulated and measured channel data," *Elec. Letters*, vol. 37, no. 18, pp. 1137–1139, Aug. 2001.
- [24] R. J. Piechocki, P. N. Fletcher, A. R. Nix, C. N. Canagarajah, and J. P. McGeehan, "Performance of space-time coding with HIPERLAN/2 and IEEE 802.11a wlan standards on real channels," in *Proc. Veh. Technol. Conf.*, 2001, vol. 2, pp. 848–852.
- [25] H. Huang, H. Viswanathan, and G. J. Foschini, "Achieving high data rates in CDMA systems using BLAST techniques," in *Proc. Glob. Telecom. Conf.*, 1999, vol. 5, pp. 2316–2320.
- [26] Foschini, G. J. and M. J. Gans, "On limits of wireless communications in a fading environment when using multiple antennas," *Wireless Personal Commun.*, Vol. 6, No. 3, 311–335, 1998.
- [27] Telatar, I. E., "Capacity of multi-antenna Gaussian channels," *European Trans. Tel.*, Vol. 10, No. 6, 585–595, 1999.
- [28] R. T. Derryberry, S. D. Gray, D. M. Ionescu, G. Mandyam, and B. Raghothaman, "Transmit diversity in 3G CDMA systems," *IEEE Comm. Mag.*, vol. 40, no. 4, pp. 68 –75, April 2002.
- [29] T. S. Rappaport, A. Annamalai, R. M. Buehrer, and W. H. Tranter, "Wireless communications: past events and a future perspective," *IEEE Comm. Magazine*, vol. 40, no. 5, pp. 148–161, May2002.
- [30] Shui, D. S., G. J. Foschini, M. J. Gans, and J. M. Kahn, "Fading correlation and its effect on the capacity of multielement antenna systems," *IEEE Trans. on Commun.*, Vol. 48, No. 3, 502–513, 2000.
- [31] McNamara, D. P., M. A. Beach, and P. N. Fletcher, "Spatial correlation in indoor MIMO channels," *Proc. of IEEE Personal Indoor and Mobile Radio Communications*, Vol. 1, 290–294, 2002. [32]Forenza, A. and R. W. Heath Jr., "Impact of antenna geometry on MIMO communication in indoor clustered

channels,” *Proc. Of IEEE Antennas and Propagation Symposium*, Vol. 2, 1700–1703, 2004.

[33] Saleh, A. A. M. and R. A. Valenzuela, “A statistical model for indoor multipath propagation,” *IEEE Journal on Selected Areas in Commun.*, Vol. 5, No. 2, 128–137, 1987. [34] Andersen, J. B. and B. N. Getu, “The MIMO cube — a compact MIMO antenna,” *Proc. of IEEE Wireless Personal Multimedia Commun.*, Vol. 1, 112–114, 2002.

[35] Abouda, A. A, N. G. Tarhuni, and H. M. El-Sallabi, “Modelbased investigation on MIMO channel capacity in main street of urban microcells,” *Proc. of IEEE Antennas and Propagation Symposium*, 313–316, 2005.

# Appendix A

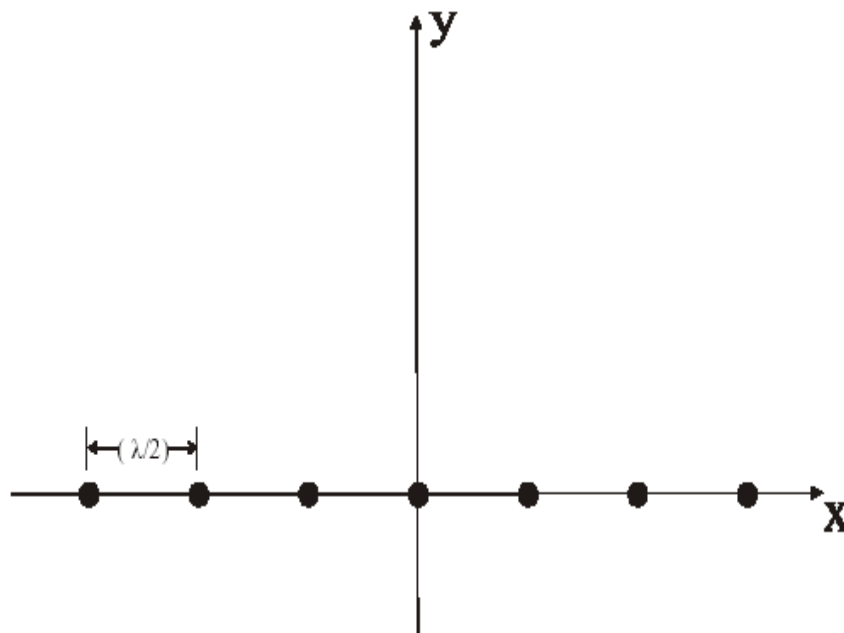
## Antenna Array Geometries used in the Simulation

For simulation purpose 5 different array configurations were used. They are,

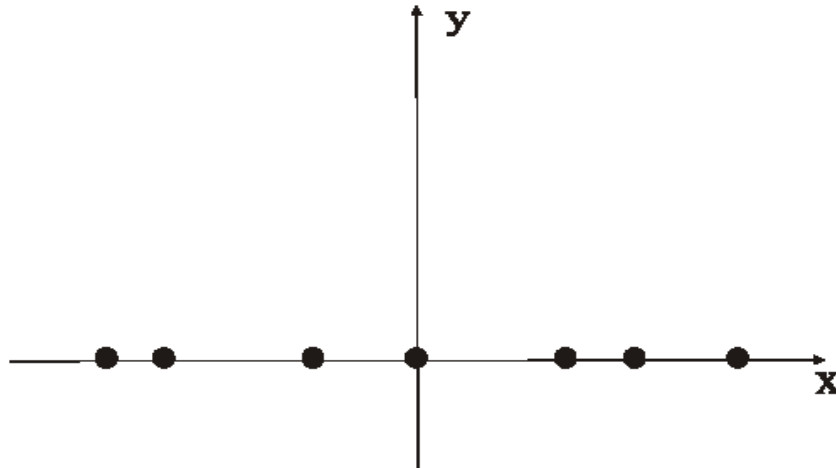
- a. Uniform Linear Array
- b. Non-Uniform Linear Array
- c. Uniform Circular Array
- d. Hexagonal Array
- e. Star Array

The array configurations are given in this appendix. Number of elements in the array is taken to be 7 and inter-element spacing is half wavelength ( $\lambda/2$ ).

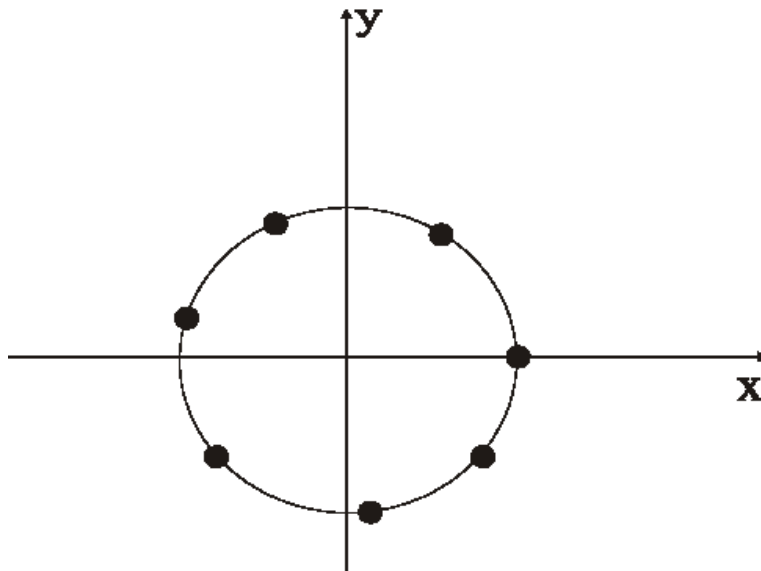
### a. Uniform Linear Array



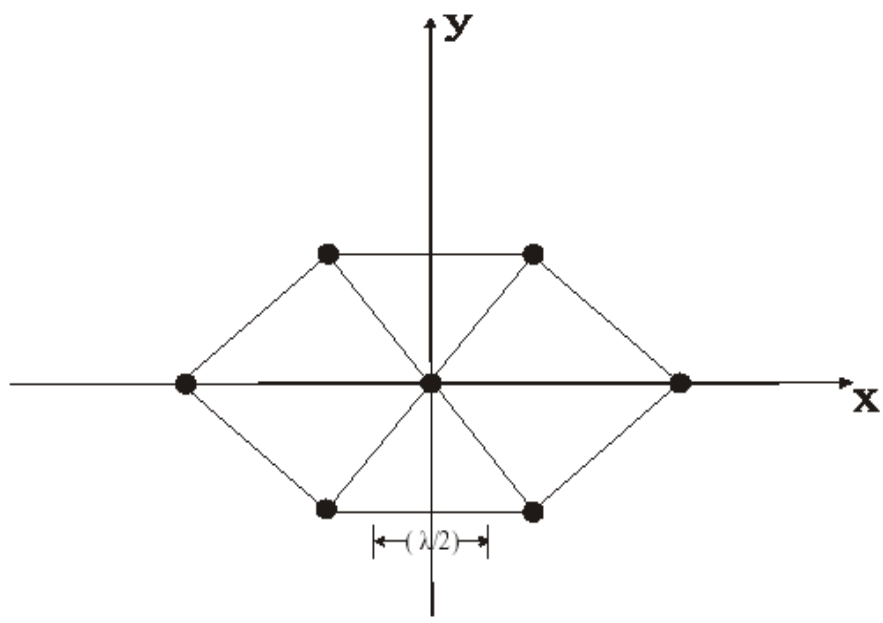
**b. Non-Uniform Linear Array**



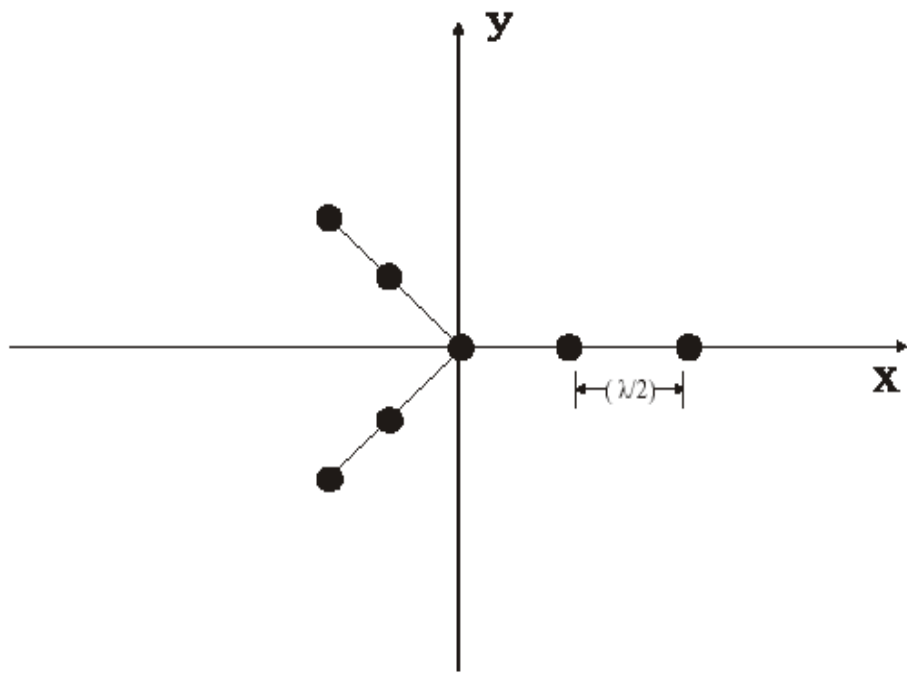
**c. Uniform Circular Array**



**d. Hexagonal Array**



e. Star Array



# Appendix B

## Simulation Codes

### B.1 Code for array manifold vector

```
%=====
=====
```

```
function [S]=sspv(m,n)
clear all
pro0=1000;
for i=1:length(m)
S = (pro0/(sqrt(m(:,i)*m(:,i) - 2*pro0*n'*m(:,i) + pro0^2))) * exp(-2*j*pi *
(sqrt(m(:,i)*m(:,i) - 2*pro0*n'*m(:,i) + pro0^2) - pro0));
End
```

```
%=====
=====
```

### B.2 Code for Section 4.2.1

```
%=====
% SIVO system without using Beamforming techniques.
% No of element at the transmitter is 1 and that at the receiver is 7
% Transmitter and receiver positioned at 1000 unit apart (in half wavelength)
% inter-element spacing half wavelength.
%=====
```

```
clear all % clear all the workspace variables
```

```

norm_d = 1; % inter-element spacing
Mt = 1; % no of elements in the transmitter
Mr = 7; % no of elements in the receiver
ro = 1000; % distance between source and receiver
s_power = 9*10^5; % signal power
d_AoA = 71; % angle of arrival for desired user
SNR = [0, 5, 10, 15, 20, 25, 30, 35, 40];
% Fading Coefficients=====
beta = sqrt(s_power)*(1/ro)*exp(j*2*pi*ro);
%Source Directions=====
for i = 0:180
directions(i+1,:) = [i, 0];
end
% Antenna Geometry=====
%Uniform Linear Array=====
array_ULA = [ -3*norm_d 0 0;-2*norm_d 0 0;-1*norm_d 0 0;0 0 0;norm_d 0
0;2*norm_d 0 0;3*norm_d 0 0 ];
%Non-Uniform Linear Array=====
array_NULA = [ -1.80 0 0;-1.55 0 0;-1.30 0 0;-1.15 0 0;0 0 0;1.10 0 0;1.20 0 0 ];
%Uniform Circular Array=====
for i = 0:(Mr-1)
array_UCA(i+1,:) = [ cos(i*2*pi/Mr) sin(i*2*pi/Mr) 0];
end
%Hexagonal Array=====
array_HA = [ norm_d*cos((pi/180)*180) norm_d*sin((pi/180)*180)
0;norm_d*cos((pi/180)*225) norm_d*sin((pi/180)*225)
0;norm_d*cos((pi/180)*135) norm_d*sin((pi/180)*135) 0;0 0
0;norm_d*cos((pi/180)*315) norm_d*sin((pi/180)*315) 0;norm_d*cos((pi/180)*45)
norm_d*sin((pi/180)*45) 0;norm_d*cos((pi/180)*0) norm_d*sin((pi/180)*0) 0 ];

```

```

%Star Array=====
array_SA = [ 2*norm_d*cos((pi/180)*120) 2*norm_d*sin((pi/180)*120)
0;2*norm_d*cos((pi/180)*240) 2*norm_d*sin((pi/180)*240)
0;norm_d*cos((pi/180)*120) norm_d*sin((pi/180)*120)
0;norm_d*cos((pi/180)*240) norm_d*sin((pi/180)*240) 0;0 0
0;norm_d*cos((pi/180)*0) norm_d*sin((pi/180)*0) 0;2*norm_d*cos((pi/180)*0)
2*norm_d*sin((pi/180)*0) 0 ];

```

```

%Manifold Vector=====

```

```

% Uniform Linear Array=====

```

```

for i = 1:length(directions)
s_location = [directions(i,:) ro];
array = array_ULA';
s=s_location';
S_ULA(:,i) = sspv(array, s);
end

```

```

% Non-Uniform Linear Array=====

```

```

for i = 1:length(directions)
s_location = [directions(i,:) ro];
array = array_NULA';
s=s_location';
S_NULA(:,i) = sspv(array, s);
end

```

```

% Uniform Circular Array=====

```

```

for i = 1:length(directions)
s_location = [directions(i,:) ro];
array = array_UCA';
s=s_location';
S_UCA(:,i) = sspv(array, s);

```

```

end

% Hexagonal Array=====
for i = 1:length(directions)
s_location = [directions(i,:) ro];
array = array_HA';
s=s_location';
S_HA(:,i) = sspv(array, s);
end

% Star Array=====
for i = 1:length(directions)
s_location = [directions(i,:) ro];
array = array_SA';
s=s_location';
S_SA(:,i) = sspv(array, s);
end

% Channel Matrix=====
H_ULA = S_ULA*beta;
H_NULA = S_NULA*beta;
H_UCA = S_UCA*beta;
H_HA = S_HA*beta;
H_SA = S_SA*beta;

% Capacity=====
Uniform Linear Array=====
for i = 1 :length(directions)
for k = 1:length(SNR)
snr = 10^(SNR(k)/10);
C_ULA(k,i) = 0.5*log2(det(eye(Mr)+(snr/Mt)*H_ULA(:,i)*H_ULA(:,i)'));
end
end
end

```

```

%Non-Uniforma Linear Array=====
for i = 1:length(directions)
for k = 1:length(SNR)
snr = 10^(SNR(k)/10);
C_NULA(k,i) = 0.5*log2(det(eye(Mr)+(snr/Mt)*H_NULA(:,i)*H_NULA(:,i)'));
end
end
%Uniforma Circular Array=====
for i = 1:length(directions)
for k = 1:length(SNR)
snr = 10^(SNR(k)/10);
C_UCA(k,i) = 0.5*log2(det(eye(Mr)+(snr/Mt)*H_UCA(:,i)*H_UCA(:,i)'));
end
end
%Hexagonal Array=====
for i = 1:length(directions)
for k = 1:length(SNR)
snr = 10^(SNR(k)/10);
C_HA(k,i) = 0.5*log2(det(eye(Mr)+(snr/Mt)*H_HA(:,i)*H_HA(:,i)'));
end
end
%Star Array=====
for i = 1:length(directions)
for k = 1:length(SNR)
snr = 10^(SNR(k)/10);
C_SA(k,i) = 0.5*log2(det(eye(Mr)+(snr/Mt)*H_SA(:,i)*H_SA(:,i)'));
end
end
end
%plots=====
surf(directions(:,1),SNR,abs(C_ULA));

```

```
ylabel('SNR (dB)');  
xlabel('Angle of Arrival (deg)');  
zlabel('capacity (bits/sec/Hz)');  
title('Impact of SNR and AoA on Capacity using Uniform Linear Array');
```

```
figure  
surf(directions(:,1),SNR,abs(C_NULA));  
ylabel('SNR (dB)');  
xlabel('Angle of Arrival (deg)');  
zlabel('capacity (bits/sec/Hz)');  
title('Impact of SNR and AoA on Capacity using Non-Uniform Linear Array');
```

```
figure  
surf(directions(:,1),SNR,abs(C_UCA));  
ylabel('SNR (dB)');  
xlabel('Angle of Arrival (deg)');  
zlabel('capacity (bits/sec/Hz)');  
title('Impact of SNR and AoA on Capacity using Uniform Circular Array');
```

```
figure  
surf(directions(:,1),SNR,abs(C_HA));  
ylabel('SNR (dB)');  
xlabel('Angle of Arrival (deg)');  
zlabel('capacity (bits/sec/Hz)');  
title('Impact of SNR and AoA on Capacity using Hexagonal Array');
```

```
figure  
surf(directions(:,1),SNR,abs(C_SA));  
ylabel('SNR (dB)');  
xlabel('Angle of Arrival (deg)');
```

```
zlabel('capacity (bits/sec/Hz)');
title('Impact of SNR and AoA on Capacity using Star Array');
```

```
figure
plot(SNR,abs(C_SA(:,d_AoA)),'-xk',SNR,abs(C_HA(:,d_AoA)),'-
.b',SNR,abs(C_UCA(:,d_AoA)),'-or',SNR,abs(C_NULA(:,d_AoA)),'-
sg',SNR,abs(C_ULA(:,d_AoA)),'-ok');
legend('Star Array','Hexagonal Array','Uniform Circular Array','Non-Uniform
Linear Array','Uniform Linear Array');
xlabel('SNR (dB)');
ylabel('Capacity (bits/sec/Hz)');
title('Impact of Antenna Geometry on Capacity');
grid on
grid minor
```

```
%=====
```

### B.3 code for section 4.2.2

Code for Uniform Linear Array

```
% =====
% SIVO system without using Beamforming techniques.
% No of element at the transmitter is 1 and that at the receiver is 7
% Transmitter and receiver positioned at 1000 unit apart (in half wavelength)
% inter-element spacing half wavelength.
% =====
clear all % clear all the workspace variables
normal_d = 1; % inter-element spacing
```

```

Mt = 1; % no of elements in the transmitter
Mr = 7; % no of elements in the receiver
ro = 1000; % distance between source and receiver
s_power = 9*10^5; % signal power
d_AoA = 71; % angle of arrival for desired user
SNR = [0, 5, 10, 15, 20, 25, 30, 35, 40];

% Fading Coefficients=====
beta = sqrt(s_power)*(1/ro)*exp(j*2*pi*ro);
%Source Directions=====
for i = 0:180
directions(i+1,:) = [i, 0];
end
% Antenna Geometry=====
%Uniform Linear Array=====
% # of Elements : 7=====
array_ULA_7 = [-3*norm_d 0 0;
-2*norm_d 0 0;
-1*norm_d 0 0;
0 0 0;
norm_d 0 0;
2*norm_d 0 0;
3*norm_d 0 0 ];
% # of Elements : 6=====
array_ULA_6 = [-2.5*norm_d 0 0;
-1.5*norm_d 0 0;
-0.5*norm_d 0 0;
0.5*norm_d 0 0;
1.5*norm_d 0 0;
2.5*norm_d 0 0 ];

```

```

% # of Elements : 5=====
array_ULA_5 = [-2*norm_d 0 0;
-1*norm_d 0 0;
0 0 0;
norm_d 0 0;
2*norm_d 0 0 ];

% # of Elements : 4=====
array_ULA_4 = [-1.5*norm_d 0 0;
-0.5*norm_d 0 0;
0.5*norm_d 0 0;
1.5*norm_d 0 0 ];
% # of Elements : 3=====
array_ULA_3 = [-1*norm_d 0 0;
0 0 0;
norm_d 0 0 ];
%Manifold Vector=====
% Uniform Linear Array 7=====
for i = 1:length(directions)
s_location = [directions(i,:) ro];
S_ULA_7(:,i) = sspv(array_ULA_7, s_location);
end
% Uniform Linear Array 6=====
for i = 1:length(directions)
s_location = [directions(i,:) ro];
S_ULA_6(:,i) = sspv(array_ULA_6, s_location);
end
% Uniform Linear Array 6=====
for i = 1:length(directions)
s_location = [directions(i,:) ro];

```

```

S_ULA_5(:,i) = sspv(array_ULA_5, s_location);
end
% Uniform Linear Array 4=====
for i = 1:length(directions)
s_location = [directions(i,:) ro];
S_ULA_4(:,i) = sspv(array_ULA_4, s_location);
end

% Uniform Linear Array 3=====
for i = 1:length(directions)
s_location = [directions(i,:) ro];
S_ULA_3(:,i) = sspv(array_ULA_3, s_location);
end
% Channel matrix=====
H_ULA_7 = S_ULA_7*beta; %% Uniform Linear Array #7
H_ULA_6 = S_ULA_6*beta; %% Uniform Linear Array #6
H_ULA_5 = S_ULA_5*beta; %% Uniform Linear Array #5
H_ULA_4 = S_ULA_4*beta; %% Uniform Linear Array #4
H_ULA_3 = S_ULA_3*beta; %% Uniform Linear Array #3
% Capacity=====
% Uniform Linear Array 7=====
for i = 1:length(directions)
for k = 1:length(SNR)
snr = 10^(SNR(k)/10);
C_ULA_7(k,i) = log2(det(eye(7)+(snr/Mt)*H_ULA_7(:,i)*H_ULA_7(:,i)));
end
end
% Uniform Linear Array 6=====
for i = 1:length(directions)
for k = 1:length(SNR)

```

```

snr = 10^(SNR(k)/10);
C_ULA_6(k,i) = log2(det(eye(6)+(snr/Mt)*H_ULA_6(:,i)*H_ULA_6(:,i)));
end
end
% Uniform Linear Array 5=====
for i = 1:length(directions)
for k = 1:length(SNR)
snr = 10^(SNR(k)/10);
C_ULA_5(k,i) = log2(det(eye(5)+(snr/Mt)*H_ULA_5(:,i)*H_ULA_5(:,i)));
end
end
% Uniform Linear Array 4=====
for i = 1:length(directions)
for k = 1:length(SNR)
snr = 10^(SNR(k)/10);
C_ULA_4(k,i) = log2(det(eye(4)+(snr/Mt)*H_ULA_4(:,i)*H_ULA_4(:,i)));
end
end
% Uniform Linear Array 3=====
for i = 1:length(directions)
for k = 1:length(SNR)
snr = 10^(SNR(k)/10);
C_ULA_3(k,i) = log2(det(eye(3)+(snr/Mt)*H_ULA_3(:,i)*H_ULA_3(:,i)));
end
end
% plots=====
plot(SNR,abs(C_ULA_7(:,d_AoA)),-xr.,
SNR,abs(C_ULA_6(:,d_AoA)),-ok.,
SNR,abs(C_ULA_5(:,d_AoA)),-oc.,
SNR,abs(C_ULA_4(:,d_AoA)),-sm.,

```

```

SNR,abs(C_ULA_3(:,d_AoA)),.-+k.);
legend(.Uniform Linear Array #7.,.Uniform Linear Array #6.,
Uniform Linear Array #5.,.Uniform Linear Array #4.,
Uniform Linear Array #3.);
xlabel(.SNR (dB).);
C. Simulation Codes 81
ylabel(.Capacity (bits/sec/Hz).);
title(.Impact of Antenna Geometry on Capacity.);
grid on
grid minor
%=====

```

#### **B.4 Code for Uniform Circular Array**

```

% =====
% SIVO system without using Beamforming techniques.
% No of element at the transmitter is 1 and that at the receiver is 7
% Transmitter and receiver positioned at 1000 unit apart (in half wavelength)
% inter-element spacing half wavelength.
% =====
clear all % clear all the workspace variables
normal_d = 1; % inter-element spacing
Mt = 1; % no of elements in the transmitter
Mr = 7; % no of elements in the receiver
ro = 1000; % distance between source and receiver
s_power = 9*10^5; % signal power
d_AoA = 71; % angle of arrival for desired user
SNR = [0, 5, 10, 15, 20, 25, 30, 35, 40];
% Fading Coefficients=====
beta = sqrt(s_power)*(1/ro)*exp(j*2*pi*ro);

```

```

%Source Directions=====
for i = 0:180
directions(i+1,:) = [i, 0];
end
% Antenna Geometry=====
%Uniform Circular Array=====
% # of Elements : 7=====
for i = 0:(Mr-1)
array_UCA_7(i+1,:) = [ cos(i*2*pi/Mr) sin(i*2*pi/Mr) 0];
end
% # of Elements : 6=====
for i = 0:(Mr-2)
array_UCA_6(i+1,:) = [ cos(i*2*pi/Mr) sin(i*2*pi/Mr) 0];
end
% # of Elements : 5=====
for i = 0:(Mr-3)
array_UCA_5(i+1,:) = [ cos(i*2*pi/Mr) sin(i*2*pi/Mr) 0];
end
% # of Elements : 4=====
for i = 0:(Mr-4)
array_UCA_4(i+1,:) = [ cos(i*2*pi/Mr) sin(i*2*pi/Mr) 0];
end
% # of Elements : 3=====
for i = 0:(Mr-5)
array_UCA_3(i+1,:) = [ cos(i*2*pi/Mr) sin(i*2*pi/Mr) 0];
end
%Manifold Vector=====
% Uniform Circular Array 7=====
for i = 1:length(directions)
s_location = [directions(i,:) ro];

```

```

array = array_UCA_7';
s=s_location';
S_UCA_7(:,i) = sspv(array, s);
end
% Uniform Circular Array 6=====
for i = 1:length(directions)
s_location = [directions(i,:) ro];
array = array_UCA_6';
s=s_location';
S_UCA_6(:,i) = sspv(array, s);
end
% Uniform Circular Array 5=====
for i = 1:length(directions)
s_location = [directions(i,:) ro];
array = array_UCA_5';
s=s_location';
S_UCA_5(:,i) = sspv(array, s);
end
% Uniform Circular Array 4=====
for i = 1:length(directions)
s_location = [directions(i,:) ro];
array = array_UCA_4';
s=s_location';
S_UCA_4(:,i) = sspv(array, s);
end
% Uniform Circular Array 3=====
for i = 1:length(directions)
s_location = [directions(i,:) ro];
array = array_UCA_3';
s=s_location';

```

```

S_UCA_3(:,i) = sspv(array, s);
end
% Channel matrix=====
H_UCA_7 = S_UCA_7*beta; %% Uniform Linear Array #7
H_UCA_6 = S_UCA_6*beta; %% Uniform Linear Array #6
H_UCA_5 = S_UCA_5*beta; %% Uniform Linear Array #5
H_UCA_4 = S_UCA_4*beta; %% Uniform Linear Array #4
H_UCA_3 = S_UCA_3*beta; %% Uniform Linear Array #3
% Capacity=====
% Uniform Circular Array 7=====
for i = 1:length(directions)
for k = 1:length(SNR)
snr = 10^(SNR(k)/10);
C_UCA_7(k,i) = log2(det(eye(7)+(snr/Mt)*H_UCA_7(:,i)*H_UCA_7(:,i)'));
end
end
% Uniform Circular Array 6=====
for i = 1:length(directions)
for k = 1:length(SNR)
snr = 10^(SNR(k)/10);
C_UCA_6(k,i) = log2(det(eye(6)+(snr/Mt)*H_UCA_6(:,i)*H_UCA_6(:,i)'));
end
end
% Uniform Circular Array 5=====
for i = 1:length(directions)
for k = 1:length(SNR)
snr = 10^(SNR(k)/10);
C_UCA_5(k,i) = log2(det(eye(5)+(snr/Mt)*H_UCA_5(:,i)*H_UCA_5(:,i)'));
end
end
end

```

```

% Uniform Circular Array 4=====
for i = 1:length(directions)
for k = 1:length(SNR)
snr = 10^(SNR(k)/10);
C_UCA_4(k,i) = log2(det(eye(4)+(snr/Mt)*H_UCA_4(:,i)*H_UCA_4(:,i)'));
end
end
% Uniform Circular Array 3=====
for i = 1:length(directions)
for k = 1:length(SNR)
snr = 10^(SNR(k)/10);
C_UCA_3(k,i) = log2(det(eye(3)+(snr/Mt)*H_UCA_3(:,i)*H_UCA_3(:,i)'));
end
end

% plots=====
plot(SNR,abs(C_UCA_7(:,d_AoA)),'-xr',SNR,abs(C_UCA_6(:,d_AoA)),'-
ok',SNR,abs(C_UCA_5(:,d_AoA)),'-oc',SNR,abs(C_UCA_4(:,d_AoA)),'-
sm',SNR,abs(C_UCA_3(:,d_AoA)),'-+k');
legend('Uniform Circuler Array #7','Uniform Circuler Array #6','Uniform Circuler
Array #5','Uniform Circuler Array #4','Uniform Circuler Array #3');
xlabel('SNR (dB)');
ylabel('Capacity (bits/sec/Hz)');
title('Impact of Antenna Geometry on Capacity');
grid on
grid minor

%=====

```

## B.5 Code for Star Array

```
% =====  
% SIVO system without using Beamforming techniques.  
% No of element at the transmitter is 1 and that at the receiver is 7  
% Transmitter and receiver positioned at 1000 unit apart (in half wavelength)  
% inter-element spacing half wavelength.  
% =====  
clear all % clear all the workspace variables  
norm_d = 1; % inter-element spacing  
Mt = 1; % no of elements in the transmitter  
Mr = 7; % no of elements in the receiver  
ro = 1000; % distance between source and receiver  
s_power = 9*10^5; % signal power  
d_AoA = 71; % angle of arrival for desired user  
SNR = [0, 5, 10, 15, 20, 25, 30, 35, 40];  
% Fading Coefficients=====  
beta = sqrt(s_power)*(1/ro)*exp(j*2*pi*ro);  
%Source Directions=====  
for i = 0:180  
directions(i+1,:) = [i, 0];  
end  
  
% Antenna Geometry=====  
%Star Array=====  
% # of Elements : 7=====  
array_SA_7 = [ 2*norm_d*cos((pi/180)*120) 2*norm_d*sin((pi/180)*120) 0;  
2*norm_d*cos((pi/180)*240) 2*norm_d*sin((pi/180)*240) 0;  
norm_d*cos((pi/180)*120) norm_d*sin((pi/180)*120) 0;  
norm_d*cos((pi/180)*240) norm_d*sin((pi/180)*240) 0;
```

```

0 0 0;
norm_d*cos((pi/180)*0) norm_d*sin((pi/180)*0) 0;
2*norm_d*cos((pi/180)*0) 2*norm_d*sin((pi/180)*0) 0 ];
% # of Elements : 6=====
array_SA_6 = [ 2*norm_d*cos((pi/180)*240) 2*norm_d*sin((pi/180)*240) 0;
norm_d*cos((pi/180)*120) norm_d*sin((pi/180)*120) 0;
norm_d*cos((pi/180)*240) norm_d*sin((pi/180)*240) 0;
0 0 0;
norm_d*cos((pi/180)*0) norm_d*sin((pi/180)*0) 0;
2*norm_d*cos((pi/180)*0) 2*norm_d*sin((pi/180)*0) 0 ];
% # of Elements : 5=====
array_SA_5 = [ norm_d*cos((pi/180)*120) norm_d*sin((pi/180)*120) 0;
norm_d*cos((pi/180)*240) norm_d*sin((pi/180)*240) 0;
0 0 0;
norm_d*cos((pi/180)*0) norm_d*sin((pi/180)*0) 0;
2*norm_d*cos((pi/180)*0) 2*norm_d*sin((pi/180)*0) 0 ];

% # of Elements : 4=====
array_SA_4 = [ norm_d*cos((pi/180)*240) norm_d*sin((pi/180)*240) 0;
0 0 0;
norm_d*cos((pi/180)*0) norm_d*sin((pi/180)*0) 0;
2*norm_d*cos((pi/180)*0) 2*norm_d*sin((pi/180)*0) 0 ];
% # of Elements : 3=====
array_SA_3 = [ norm_d*cos((pi/180)*240) norm_d*sin((pi/180)*240) 0;
0 0 0;
norm_d*cos((pi/180)*0) norm_d*sin((pi/180)*0) 0];
%Manifold Vector=====
% Star Array 7=====
for i = 1:length(directions)
s_location = [directions(i,:) ro];

```

```

array = array_SA_7';
s=s_location';
S_SA_7(:,i) = sspv(array, s);
end
% Star Array 6=====
for i = 1:length(directions)
s_location = [directions(i,:) ro];
array = array_SA_6';
s=s_location';
S_SA_6(:,i) = sspv(array, s);
end
% Star Array 5=====
for i = 1:length(directions)
s_location = [directions(i,:) ro];
array = array_SA_5';
s=s_location';
S_SA_5(:,i) = sspv(array, s);
end
% Star Array 4=====
for i = 1:length(directions)
s_location = [directions(i,:) ro];
array = array_SA_4';
s=s_location';
S_SA_4(:,i) = sspv(array, s);
end
% Star Array 3=====
for i = 1:length(directions)
s_location = [directions(i,:) ro];
array = array_SA_3';
s=s_location';

```

```

S_SA_3(:,i) = sspv(array, s);
end
% Channel matrix=====
H_SA_7 = S_SA_7*beta; %% Uniform Linear Array #7
H_SA_6 = S_SA_6*beta; %% Uniform Linear Array #6
H_SA_5 = S_SA_5*beta; %% Uniform Linear Array #5
H_SA_4 = S_SA_4*beta; %% Uniform Linear Array #4
H_SA_3 = S_SA_3*beta; %% Uniform Linear Array #3
% Capacity=====
% Star Array 7=====
for i = 1:length(directions)
for k = 1:length(SNR)
snr = 10^(SNR(k)/10);
C_SA_7(k,i) = log2(det(eye(7)+(snr/Mt)*H_SA_7(:,i)*H_SA_7(:,i)'));
end
end
% Star Array 6=====

for i = 1:length(directions)
for k = 1:length(SNR)
snr = 10^(SNR(k)/10);
C_SA_6(k,i) = log2(det(eye(6)+(snr/Mt)*H_SA_6(:,i)*H_SA_6(:,i)'));
end
end
% Star Array 5=====
for i = 1:length(directions)
for k = 1:length(SNR)
snr = 10^(SNR(k)/10);
C_SA_5(k,i) = log2(det(eye(5)+(snr/Mt)*H_SA_5(:,i)*H_SA_5(:,i)'));
end
end

```

```

end
% Star Array 4=====
for i = 1:length(directions)
for k = 1:length(SNR)
snr = 10^(SNR(k)/10);
C_SA_4(k,i) = log2(det(eye(4)+(snr/Mt)*H_SA_4(:,i)*H_SA_4(:,i)'));
end
end
% Star Array 3=====
for i = 1:length(directions)
for k = 1:length(SNR)
snr = 10^(SNR(k)/10);
C_SA_3(k,i) = log2(det(eye(3)+(snr/Mt)*H_SA_3(:,i)*H_SA_3(:,i)'));
end
end

% plots=====
plot(SNR,abs(C_SA_7(:,d_AoA)),'-xr',SNR,abs(C_SA_6(:,d_AoA)),'-
ok',SNR,abs(C_SA_5(:,d_AoA)),'-oc',SNR,abs(C_SA_4(:,d_AoA)),'-
sm',SNR,abs(C_SA_3(:,d_AoA)),'-+k');
legend('Star Array #7','Star Array #6','Star Array #5','Star Array #4','Star Array
#3');
xlabel('SNR (dB)');
ylabel('Capacity (bits/sec/Hz)');
title('Impact of Antenna Geometry on Capacity');
grid on
grid minor
%=====

```

